arXiv:1511.06307v3 [gr-qc] 10 Jun 2016

Equivalence Principle in Chameleon Models

Lucila Kraiselburd,[1] Susana J. Landau,[2] Marcelo Salgado,[3] Daniel Sudarsky,[4] and Héctor Vucetich[5]

[1] *Grupo de Astrofísica, Relatividad y Cosmología, Facultad de Ciencias Astronómicas y Geofísicas, Universidad Nacional de La Plata and CONICET, Paseo del Bosque S/N (1900) La Plata, Argentina**

[2] *Departamento de Física, Facultad de Ciencias Exactas y Naturales, Universidad de Buenos Aires and IFIBA, CONICET, Ciudad Universitaria - Pab. I, Buenos Aires 1428, Argentina*†

[3] *Instituto de Ciencias Nucleares, Universidad Nacional Autónoma de México, A. Postal 70-543, México D.F. 04510, México.*‡

[4] *Instituto de Ciencias Nucleares, Universidad Nacional Autónoma de México, A. Postal 70-543, México D.F. 04510, México*§

[5] *Grupo de Astrofísica, Relatividad y Cosmología, Facultad de Ciencias Astronómicas y Geofísicas, Universidad Nacional de La Plata, Paseo del Bosque S/N (1900) La Plata, Argentina.*¶

Most theories that predict time and/or space variation of fundamental constants also predict violations of the Weak Equivalence Principle (WEP). Khoury and Weltman proposed the chameleon model in 2004 and claimed that this model avoids experimental bounds on the WEP. In this paper we present a contrasting view based on the analysis of the force between *two bodies induced by the chameleon field* using a particular approach in which the field due to both the *large* and the *small* bodies is obtained by appropriate series expansions in the various regions of interest and the corresponding matching conditions. We found that resulting force depends on the test body's composition even when the chameleon coupling constants $\beta^i = \beta$ are universal. In particular, we compared the resulting differential acceleration of test bodies made of Be and Al with the corresponding bounds obtained from Eötvös type experiments and find that the predictions of the chameleon model are, in general, various orders of magnitude above the current bounds. These results strongly suggest that the properties of immunity from experimental test of the equivalence principle usually attributed to the chameleon and related models, should be carefully reconsidered. However, it is important to mention that the new bounds depend strongly on the detailed geometry of the experiment considered. For instance, the chameleon force can be exponentially suppressed if the instrument is encased by a *symmetric* shell of a dense material as opposed to vacuum or the terrestrial atmosphere. In that case, the allowed coupling can be as large as $\beta > 10^{-2}$. On the other hand, "two body" experiments not screened by a dense shell material, such as space-based test of the WEP like the Lunar-laser ranging, can provide further constraints on the values of the model's parameters over those that might be obtained from a terrestrial "two body" instrument surrounded by a low-density material.

I. INTRODUCTION

The Weak Equivalence Principle (WEP) is a cornerstone of the Einstein's Theory of General Relativity (hereafter GR), and can be broadly seen as implying the universal coupling between matter and gravity. On the other hand, any theory in which the local coupling constants become effectively spacetime dependent, while respecting the principles of locality and general covariance, will entail some kind of fundamental field controlling such dependence, and coupling in different manners to the various types of matter. Such field, usually taken to be a scalar field, will generically mediate new forces between *macroscopic* objects, which would look, at the empirical level, as modifications of gravitation which might, in principle, lead to effective violations of the universality of free fall for *test* bodies in external gravitational fields. For this reason, most theories that predict variations of fundamental constants also predict effective violations of the WEP [1–5]. The point is that the rest energy of a macroscopic body is made of many contributions related

*Electronic address: lkrai@fcaglp.unlp.edu.ar
†Electronic address: slandau@df.uba.ar
‡Electronic address: marcelo@nucleares.unam.mx
§Electronic address: sudarsky@nucleares.unam.mx
¶Electronic address: vucetich@fcaglp.unlp.edu.ar

to the energies associated with various kinds of interactions (strong, weak, electromagnetic) and such components would be affected differently by the light scalar field. From the experimental point of view, we must thus consider the very strong limits on possible violations of the WEP that come from Eötvös-Roll-Krotkov-Dicke and Braginsky-Panov experiments and their modern reincarnations [6–11] which explore the differential acceleration of test bodies. In fact the latest bounds give $\frac{\Delta a}{a} \simeq 10^{-13}$, severely constraining the viability of many models. In the most precise kind of experiments on this line, a continuously rotating torsion balance instrument is used to measure the acceleration difference toward a large source (like the Earth, a lake, or a mountain) of test bodies with the same mass but different composition.

Recently, there has been a great level of interest in models that claim to be able to avoid the stringent bounds resulting from experimental tests looking for violations WEP based on schemes where the fields hide their effects as the chameleon models and the Dilaton-Matter-gravity model with strong coupling [12]. Chameleon models were introduced by Khoury and Weltman in 2004 [13] and have been further developed by several authors [14–16]. Generically a *chameleon* consists of a scalar field that is coupled non-minimally to matter and minimally to the curvature (or the other way around via a conformal transformation), and where the field's effective mass depends on the density and pressure of the matter that constitutes the *environment*. This, in turn, is a result of the nontrivial coupling of the scalar field with the trace of the energy-momentum tensor of the matter sector of the theory [1]. The coupling of the scalar field with matter might be *non-universal*, like in the original model introduced in [13], or universal as in some simpler models.

Khoury and Weltman analyzed the solution of the chameleon in the *pseudolinear* approximation[2], and then corroborated that the approximate solution looks very similar to the numerical solution using the full non-linear chameleon equation. Their conclusion was that the bounds imposed by the experiments testing the WEP can be satisfied (even if the coupling constants are of order unity) provided that the bodies involved in the relevant experiments, generate the so called *thin shell effect*. In this "thin-shell" regime, the spatial variations of the scalar field take place just on a small region near the body's surface thus preventing the scalar field from actually exerting any force on most of the body. A further analysis by Mota and Shaw [16] strengthened the conclusion that these non linearities inherent to the chameleon models are, in fact, responsible for suppressing the effective violation of WEP in the actual experiments even when the coupling constants are very large, and not just when they are of order unity as it was initially thought [13] [3]. Moreover, the same authors point out that the predicted effective violations of the WEP in low density environments (like in space-based laboratories) can be further suppressed by adjusting the parameters of the scalar-field potential.

Based on such analyses, it has been argued, the chameleon field should not lead to any relevant sized forces in experiments on Earth that would generate a dependence on the composition of the acceleration of a falling *test* body, or in general, to any observable interaction between ordinary bodies mediated by chameleons.

We do not find these arguments to be sufficiently persuasive. The basic observation is that one could, equally well, have claimed something not entirely different by considering two macroscopic and charged conductors. It is well known that the mobility of charges in conducting materials ensure that in static situations the charges are distributed on the conductors' surface in such a way that the electric field inside strictly vanishes. Thus, except for a "thin shell" on the surface of each body, one could have argue following a similar logic as the one used in the context of the chameleon models, the external electric field could not exert forces on the conductor's material. However we of course know that large macroscopic forces between such macroscopic bodies are the rule. The resulting force could therefore be attributed solely to *thin shell* effects.

---

[1] In this context by *matter* we mean any field other that the scalar-field at hand, which in the situation of interest would be the ordinary matter making up the objects present in the experiment including the atmosphere.

[2] It is usually argued that the *chameleon* or the *thin shell* effect which is associated with the suppression of the chameleon force in agreement with the results of experimental tests of the WEP, is a high non linear effect. This seems to be in contradiction with the linearization of the chameleon equation usually encountered in the literature and as described in this paper as well (cf. Sec. II). In fact the non-linearity appears in the treatment in association with the need to linearize in different regions independently and in the required matching of the relevant solutions in each region. This is what we dub *quasilinear* approximation. This terminology is related but it is different to the one used in [16], where by *linear* they mean linearization of the chameleon equation around a certain background (more along the lines of this paper), whereas by *pseudolinear* they mean an approximation that is much similar to the one presented in Ref. [13]. So, in our "quasilinear" approach even if we linearize the chameleon equation around the three different minima of the potential associated with the interior of the two bodies and their exterior, the non-linearities that make the *thin shell* effect to appear are codified in the matching of the solutions in these regions.

[3] When analyzing the two-body problem, Mota & Shaw assumed that both bodies can be treated as two semi-infinite "blocks" in order to solve the non-linear equation for the chameleon. Several approximations led them to conclude that the force between the bodies is composition-independent. It is worthwhile noting that if one takes such approximations seriously, then the mass of both bodies would become infinite. It is then unclear what is the standard criteria in the analysis of those authors where one can neglect some issues in one approximation but at the same time take them into account at convenience.

In view of this, we proceeded to study this issue for the case of the chameleon in more detail, in order to understand what, if any, is the fundamental difference between the two situations (i.e. between the electromagnetic case and the one at hand). That is, we want to find out if the *thin shell* arguments are valid at the level of accuracy that would actually ensure the "disappearance" of the expected forces. Now before moving forward, it is worthwhile to stress two important aspects related to chameleon models: the first one is a matter of principle, and refers to the fact that, effectively the WEP is violated by construction by this kind of models, as opposed to purely metric-based theories (like GR) where the WEP is incorporated *ab initio*. That is, the WEP (for test point particles moving on geodesics) is satisfied with infinite precision in purely metric theories of gravity involving no other long range fields coupling to matter. Nevertheless, even in such metric theories the complete validity of the WEP refers only to *point test particles* which, of course, do not really exist in nature (as a result of Heisenberg's uncertainty principle). In any event, when ignoring those quantum complications, it is clear that the WEP is respected for *point test particles* in metric theories, while, in chameleon models, the WEP is violated a priori (i.e. by construction) *even* when referring to *point test particles*. As we shall see, this violation can be exacerbated when considering actual *extended test objects*. This issue is discussed in more detail below. The second aspect concerns the experiments themselves. Even if chameleon models violate by construction the WEP, those violations might not be observable in a laboratory experiment if the precision is not adequate. This means that some of the effects that might reflect these violations of the WEP can be suppressed by the thin shell phenomenon associated with the chameleon field or by the Yukawa dependence of the force associated with the effective mass of the field. Thus, as we shall illustrate within a framework of a two body problem, these violations of the WEP might be large when we consider a setting where the two bodies are embedded in a very a light medium (e.g. the vacuum or the air atmosphere) whereas they can be strongly suppressed when part of the setting (e.g. the test body) is encased in some shell of a dense material like a metal vacuum chamber.

Let us now discuss in more detail the subtle notion of a *test body* and the manner in which it will be used in the present work. This notion is crucial in metric theories and even more in theories that a priori violate the WEP because it is related with the interpretation of the actual experiments in which point test particles are only an approximation or idealization of the actual (extended) test bodies. Usually, when considering a test body or test particle one tends to think of a point-like object (rather than an extended body), and one assumes that one can safely neglect its self-gravity and any other self-field effects, as well as the back-reaction of such object as source on the background fields in the region around it. Thus, for instance, in the framework of GR, this approximation leads one to consider that such object would move along the geodesics of the background spacetime [4] (assuming of course that there are no other forces acting on the particle). On the other hand, when the self-field of the bodies under consideration cannot be neglected, one has to take into account both the body's finite size, and in principle the possible back-reaction effects on the background field. In such situation one cannot longer expect that the object would follow a geodesic of the background spacetime, and the analysis of its motion can become much more complicated [18, 20]. This issue has recently become an active field of research [21].

The recovery, starting from such a full fledged analysis, of the regime where the test body approximation would become valid is, therefore not a trivial task; and in a sense, has to be done on a one by one basis for each kind of experiment one might wish to consider, as the appropriate treatment will depend on the precision of the measurements involved. A good example of this complexity is provided by the *Ohanian drop* [22], a situation where simply going to the "zero size limit" of the drop, does not remove the effects of the local curvature of the background metric nor the self-gravitational effects. Thus, it is clear that simply taking the vanishing size limit even as the density is kept small (as compared say with that of the *larger* objects that help determine the background) is not always sufficient for the object to be suitably described as a test "point" particle .

Nevertheless, naively, and still in the framework of GR, one can generally assume that a small body with finite fixed (average) density might be considered as a test body when one is interested in its motion in the presence of a much larger body with similar or larger density. This scenario mimics the setting of some of the relevant experiments, like those designed to test the WEP, where small objects of different materials are submitted to several external forces (gravitational and centrifugal) and where one assumes one can safely ignore the back-reaction of those objects on the external field. We should note that in those cases, in contrast with the Ohanian drop, the internal restoring forces become stronger (with a negligible deformation) than those tied to any tidal effects on them due to the external and non-homogeneous gravitational field. Along this line, one expects that within the precision of the measurements, such small bodies can be considered as *bona fide* probes of the WEP, and therefore, that one is actually testing the validity of the universality of geodesic motion predicted by GR (see Appendix A for supplementary clarifications).

---

[4] When dealing with a certain class of alternative metric theories of gravity, notably, scalar-tensor theories, these geodesics define what is called the *physical metric* or the *physical frame*. That is, the physical metric is that associated with the geodesics that, according to the theory, are to be followed by point like test particles.

Turning back to the specific case of the chameleon models, things become much more complex because one needs to consider the effects of both, the gravitational field, and those of the new scalar field which might led to new long range forces.

In this work we will consider two bodies, one large and one small, with both taken as *extended* bodies. For simplicity, only the larger one will be taken to be *the source* of the gravitational field. On the other hand, regarding the chameleon field itself, we must consider the effects of the two bodies even if one of them is rather small (i.e. we analyze a two body problem as far as the chameleon is concerned, but take a one-body approximation in characterizing the gravitational field).

We will see that the force between the objects mediated by the chameleon field gives rise to a non negligible net acceleration on the smaller body. Moreover, we will show that this acceleration depends in general on the object's composition and on the free parameters of the model (here we are referring to the free parameters of the chameleon potential and to the coupling of the chameleon to matter). We conclude that, for a wide range of the model's parameters (if that model were realized in nature) this acceleration would have been observed in experimental searches for violations of the WEP. We thus find that the small and low mass body that one would usually consider as a test body cannot be reliable treated as a "point" particle in the context of chameleon models. In other words, as long as the two bodies have densities sufficiently different from the density of the ambient where they are embedded (e.g. the atmospheric density or the intergalactic medium density) and regardless of their size (provided both are actual extended objects) and their masses, the scalar field generated by the presence of the two bodies might lead to a non negligible effect on the acceleration of the lower mass body. In fact, Hui *et al.* [17] [5] using similar arguments showed that the chameleon interaction depends on the composition of the test bodies, and that this interaction can produce violations of the WEP depending on the size of the objects considered. That work focused on galactic scales rather than on laboratory experiments, concluding that small and large galaxies can fall at different rates and discussed methods to probe for such violations.

Moreover, we find that the difference in acceleration (due to the chameleon) between two small bodies of different composition under the influence of a larger body does not vanish even in the case where the chameleon coupling is universal [6], a result which seems rather counter-intuitive: that is, naively one would think that small bodies with different composition would follow the geodesic of a single (universal) Jordan-frame metric when the coupling to matter is universal (like in GR and other metric theories), and so, one might conclude that there is no reason to expect any violation of the tests of the WEP. Furthermore, when considering the situation in the Einstein-frame, where the chameleon fifth-force is manifest, the *thin shell* effect associated with the larger body should help suppress any such force and thus any observable effective violation as argued in [13], even when the coupling constants are different. The point, however, is that in the regime where the *thin shell* effect becomes relevant, the physical objects used in the experiments could not be considered as simple test bodies as far as the chameleon is concerned. That is, the strong spatial variation of the scalar field inside such bodies that is associated with the thin shell effect, implies that the effects of the object on the spacetime metric $g^{\rm J}_{\mu\nu}$ can not really be ignored. Accordingly in such situation the objects, that must be considered as extended objects, are known (even in standard general relativity) not to follow geodesics [18, 20, 21]. It is clear that in those cases, where the effects of the objects with which one probes the spacetime have non-negligible effects on the metric, one cannot argue that their motion should be independent of their structure and composition, and therefore in such cases there is no contradiction between the violation of the universality of free fall, and the fact that the coupling of matter to the spacetime metric is universal (cf. Appendix A).

Now, concerning the conflict between our conclusion and the standard expectations and arguments, it is important to note that in previous studies of the chameleons the effect of the smaller body on the scalar field was neglected. Many authors assumed that if the smaller body is on its own also in the *thin shell* regime (like in the larger body), then automatically the effect of the scalar field will be sufficiently suppressed in the two-body problem as well, and in particular that this would turn the corresponding chameleon mediated force between them essentially undetectable. As we will show this is not necessarily the case (just as in the electrostatic analogy discussed previously) and, in fact, for a wide range of the parameters of the chameleon model, small bodies of different composition will experience differential accelerations sufficiently large to be observable.

On the other hand, and in order to check the consistency of our findings, we will take the limit where the size of the test body shrinks to zero while keeping the density constant (i.e. this is the case where for a universal coupling and test point particles should not lead to any effective violation of the WEP). In doing so the mass of the test body is not kept fixed, but reduced to zero in the limiting process. Results of these calculations will verify that in this limit

---

[5] We thank P. Brax for pointing to us this reference after the first submission of the manuscript.

[6] This is the case where the couplings associated with the various matter fields take the same universal value. In this scenario all the various metrics $g^{(i)}_{\mu\nu}$ coalesce into a single metric $g^{\rm J}_{\mu\nu}$ (see Sec. II).

violations of WEP become strongly suppressed as expected (see Appendix C).

Thus, we conclude that the chameleon type of fields generically induce an empirically relevant kind of "fifth force", and that, if they were to exist, the motion of a small body would never become truly geodesic. In summary, we will see that even when the bodies involved are in the thin shell regime, and if their densities are sufficiently high, (particularly that of the smaller body), the geodesic approximation fails at the experimentally relevant level, and a WEP violating fifth force will be generically present and detectable. This conclusion may have dramatic effects regarding the viability of many modified theories of gravity that include a scalar degree of freedom which behaves like a chameleon. We shall elaborate more about this issue in our conclusions.

The paper is organized as follows. After briefly reviewing the original chameleon model in Section II, we present the method for computing the two body problem proposed in this work. We also discuss several aspects of the calculation such as the characterization of the outside medium and the importance of including the effect of vacuum's chamber shell. In Section III we compute the force on the test body and show that the force is not negligible and, to the extent that there is no protective symmetry to prevent it, it will lead to an acceleration that depends on the test body's composition. In Section IV we provide numerical results for the Eötvös parameter considering two different possibilities for the outside medium. We also show than when including the effect of the metal shell, the violations of the WEP are significatively suppressed for $\beta > 10^{-2}$. Finally, in Section V we present our conclusions and a discussion about their impact on other alternative theories of gravity. Several appendices complete the ideas of the main sections. In particular, in Appendix E we estimate the corrections to the linear approximation of the one body problem used by several authors.

II. THE MODEL

In this section we briefly review the main aspects of the chameleon model. The model involves a scalar-field Φ that couples minimally to gravity via a fiducial metric $g_{\mu\nu}$, according to the following action

$$S[g_{\mu\nu}, \Psi_m^{(i)}, \Phi] = \int d^4x\sqrt{-g}\left[\frac{M_{pl}^2}{2}R - \frac{1}{2}g^{\mu\nu}(\nabla_\mu\Phi)(\nabla_\nu\Phi) - V(\Phi)\right] - \int d^4x L_m\left(\Psi_m^{(i)}, g_{\mu\nu}^{(i)}\right), \tag{1}$$

where M_{pl} is the reduced Planck mass, R is the Ricci scalar associated with $g_{\mu\nu}$, and $\Psi_m^{(i)}$ represents schematically the different matter fields (i.e. the fields other than the chameleon Φ; for instance, all the fundamental fields of the standard model of particle physics). The potential $V(\Phi)$ is specified below. The particular feature of this action is that each specie i of matter couples *minimally* to its corresponding metric $g_{\mu\nu}^{(i)}$, while the scalar field Φ couples *non-minimally*, and in general, *non-universally* to the matter through a conformal factor that relates each metric $g_{\mu\nu}^{(i)}$ with the so called Einstein metric $g_{\mu\nu}$:

$$g_{\mu\nu}^{(i)} = \exp\left[\frac{2\beta_i\Phi}{M_{pl}}\right]g_{\mu\nu}. \tag{2}$$

Here $g_{\mu\nu}^{(i)}$ is the metric which is usually associated with the geodesics of each specie i of matter and β_i is the corresponding coupling constant between each specie and the chameleon field. For instance, when the coupling constants are universal, $\beta_i = \beta$, then the (universal) metric $g_{\mu\nu}^J = g_{\mu\nu}^{(i)}$ is called the Jordan metric, and then point particles would follow the geodesics of this metric. We will see however that a more detailed analysis indicates that even in this case, in the relevant experimental situations, that simple conclusion need not apply. Given the fact that, in general, the chameleon field couples differently to each specie of particle, this model leads to potential violations of the WEP that could in principle be explored experimentally.

Following [13, 16, 23], we consider the potential for the chameleon field to be,

$$V(\Phi) = \lambda M^{4+n}\Phi^{-n}, \tag{3}$$

where M is a constant, and n is a free parameter that can be taken to be either a positive integer or a negative even integer [cf. Eq. (12)] ($\lambda = 1$ for all values of n except when $n = -4$ where $\lambda = \frac{1}{4!}$.).

The energy-momentum tensor (EMT), $T_{\mu\nu}^{m(i)}$, for the ith matter component can be written in terms of the EMT, $T_{\mu\nu}^m$ associated with the Einstein metric as follows:

$$T_{\mu\nu}^{m(i)} = \frac{2}{\sqrt{-g^{(i)}}}\frac{\delta L_m}{\delta g_{(i)}^{\mu\nu}} = \exp\left[\frac{-2\beta_i\Phi}{M_{pl}}\right]T_{\mu\nu}^m, \tag{4}$$

where $T^m_{\mu\nu}$ is defined similarly from L_m but using the metric $g_{\mu\nu}$ instead of $g^{(i)}_{\mu\nu}$.

Consequently, the traces of both EMT's are related by

$$T^{m(i)} = g^{\mu\nu}_{(i)} T^{m(i)}_{\mu\nu} = \exp\left[\frac{-4\beta_i\Phi}{M_{pl}}\right] g^{\mu\nu} T^m_{\mu\nu} = \exp\left[\frac{-4\beta_i\Phi}{M_{pl}}\right] T^m. \tag{5}$$

Eventually, we will assume a perfect-fluid description for $T^m_{\mu\nu}$. Specifically, this perfect fluid will be taken to characterize each of two extended bodies, together with the matter constituting the environment, all of which we consider as the "source" of the chameleon field. Furthermore, in the analysis of the resulting force between the two bodies, we will simply consider a universal coupling and set $\beta_i = \beta$, in order to simplify the calculations. Hereafter, and unless otherwise indicated, all the differential operators and tensorial quantities are associated with the Einstein metric.

The equation of motion for the the chameleon Φ which arises from the action (1) is

$$\Box\Phi = \frac{\partial V_{\rm eff}}{\partial\Phi}, \tag{6}$$

where $V_{\rm eff}$ represents the effective potential defined by:

$$V_{\rm eff} = V(\Phi) - T^m \frac{\beta\Phi}{M_{pl}}, \tag{7}$$

which depends on the energy-density and pressure of the matter fields via T^m. So for the perfect fluid model, $T^m = -\rho + 3P$ which does not depend explicitly on Φ.

As we mentioned earlier, we are interested in the general static solution of Eq. (6) in the presence of two extended bodies that for simplicity we consider as spherical. We take one of them to be a very large body of mass $\mathcal{M}$ (e.g. Earth, Sun, a mountain), and the other one is a smaller body of mass $\mathcal{M}_2$ ($\mathcal{M}_2 \ll \mathcal{M}$; hereafter *test* body). In this paper we will consider for the larger body the contribution of a hillside (we will model it as a spherically symmetric body of 15.5 m radius) located at 1 m of the *test* body[7]. Both bodies are the source of the chameleon, and each one is taken to have a different but uniform density, which formally can be represented by suitable Heaviside (step) functions. Moreover, we shall consider the *quasilinear* approximation in Eq. (6) obtained by linearizing Eq. (7) around $\Phi_{\rm min}$ (associated with the minimum of $V_{\rm eff}$). This is by now a standard method of analysis of these models. We do this in each of the three mediums (i.e. the two bodies and the *environment*) and then match the solutions at the border of each of the two bodies.

The approach that we are going to use in solving this problem globally is to consider an, *in principle*, exact solution to the linearized equations, where the contribution to the field due to the presence of the two bodies is taken into account everywhere. This solution is presented for each region in the form of a series expansion which allows the characterization of the solution for the field with any desired level of precision by selecting an appropriate cutoff in this series. The approach requires an appropriate matching of the exterior and interior solutions at the boundaries of the two bodies. We neglect the back-reaction of gravity on the chameleon field, that is we will work taking the spacetime as represented by the flat background Minkowski metric. This approximation was also adopted in the original proposal [13] as well as in many other studies about the chameleon models [14–16].

The main difference between our approach and the one found in Ref. [13] (the *pseudolinear* approximation) is that they consider *ab initio* the *thin* or *thick shell* regimes. In the *thin shell* regime they find the field Φ in the following three regions which is then matched smoothly: 1) one "innermost" interior solution where $\phi(r) \approx const$; 2) one "outermost" interior solution within the thin shell which is located near the border of the body; 3) the exterior solution. On the other hand, for the *thick shell* regime, they consider only one regular interior solution and the exterior one. As we show in this section, we do not assume *a priori* that the situation corresponds to any particular regime and thus we solve the general equation both in the interior and the exterior of the bodies and then we proceed to determine the global solution by imposing the matching conditions. Hence, the *thin* or *thick shell* effects appear *naturally* (see Figs. 2 and 3 in Sect. II A) depending on the conditions of the configuration (i.e. the properties of the body and the environment).

Next, we will remind the reader the basic aspects of the the linearization procedure used to treat the effective potential for the one body problem, in order to define some quantities that will be necessary in obtaining the solution

[7] We have also considered the contribution of the Earth to the chameleon induced torque and verified that it is several orders of magnitude smaller than the corresponding torque associated with the hillside.

of the two body problem we are concerned with in this paper. Let us consider a spherically-symmetric body of radius R and density $\rho_{\rm in}$ immersed in an external medium of density $\rho_{\rm out}$. We will call this body, the *larger body*, as opposed to the *smaller body* that will be introduced later. The corresponding EMT's, $T^m_{\rm in(out)}$ are assumed to be of a perfect fluid: $T^m_{\rm in(out)} = -\rho_{\rm in(out)} + 3P_{\rm in(out)}$, where the scripts in(out) will refer to the interior (exterior) of the body, respectively. In this case we will consider two regions (interior and exterior), and since $P \ll \rho$ for non-relativistic matter, we neglect the pressure. Consequently,

$$\rho = \begin{cases} \rho_{\rm in} & r \leq R \\ \\ \rho_{\rm out} & r > R \end{cases} , \tag{8}$$

where R is the radius of the body.However, it is important to point out that the geometry of the actual Earth based experiments that have been used to test the WEP, such as those using torsion balances, is much more complex than what this simple model represents. The point is that by taking or not into account in such a modeling of an experiment each of the physical and geometrical details of the actual setup one can modify the resulting prediction of the chameleon field configuration and thus (underestimate or overestimate) the force between two bodies that one is trying to study. Specifically, different distributions of various material objects near the experiment (or as part of the experiment itself) can modify the chameleon field in a substantial way, and in addition, can distort in a considerable manner the symmetry of the problem that might be ignored in the simple modeling of such setups where those complications are absent. For instance, among such complications, we can mention the environment around the smaller body which might involve not only a vacuum or the Earth's atmosphere, but also some metal cases and other objects located in the proximity of the experimental equipment. Those complications can often be ignored when looking for linear fields coupling in a non-universal way to matter and leading to violations of the EP such as the original Fifth Force proposals [19], but that is not necessarily the case when dealing with highly non-linear models as the one studied here. In the current situation one might need in principle a very detailed model for ρ in order to take into account the true effect of the environment around the two bodies (the larger body and the test body) used to test the WEP. This would require the modeling of the matter distribution in great detail and then one faces the very difficult task of solving a complicated non-linear partial differential equation with a rather intricate boundary conditions. In order to advance in this direction and to make the calculations feasible, we are forced to abandon some of these complications while keeping some of the most important features of the experiment. For instance, we analyze the extent to which different environments affect the resulting chameleon force between the two bodies. Here we will proceed in two stages. In the first one we consider the simplest model for ρ as given by Eq. (8). First we take two type of environments represented by $\rho_{\rm out}$: one is given by the chamber's vacuum and the other is given by the Earth's atmosphere. In the second stage we estimate the correction on these results due to the encasing material around the test body. The correction to the chameleon force between the two bodies will take the form of a Yukawa-like suppression produced by the effective mass associated with the density of the shielding case which we consider to be of a spherical metal shell around the test body [8]. This suppression has been analyzed in the past by Upadhye [35] for a two body problem shielded by a dense shell where the bodies and the shell are modeled by planar slabs (as opposed to spherical like objects like in the present article) while the low density environments between the body and the shell and the shell and the test bodies are similarly modeled by planar gaps. The above setting is analyzed in [35] in a "one dimensional planar" model.

Now, in the scenario where one does not consider such metal casing, the model is meant to be applied to at least two kind of experiments: 1) a laboratory experiment which is similar to the Eöt-Wash experiment but without the metal shell; 2) an actual space-based experiment like the Lunar-laser ranging where the Sun plays the role of the larger body and the Earth or Moon represent the test bodies.

Even in the simple model where one considers just two spherical objects in a constant density environment, there are other mathematical approximations that we make in order to simplify the calculations. The first simplification consists in expanding $V_{\rm eff}(\phi)$ about its minimum in each region up to the quadratic terms and ignoring the higher order ones. We perform this analysis below. Clearly this approximation leads to a linear differential equation for the chameleon field. In the Appendix E we will estimate the corrections associated with this approximation, by considering the effects of the cubic term in the expansion as a perturbation of the one body problem [9]. We will see that the corrections become relevant for $n > 4$.

We now proceed to deal with the linear problem for the two spherical bodies in a single medium as environment.

---

[8] We thank P. Brax for calling our attention to this aspect of the experiment.
[9] We thank A. Upadhye, B.Elder and J. Khoury for raising this issue after the first submission of this manuscript

We start with the expansion of the effective potential about the corresponding minimum in each region up to the quadratic term gives:

$$V_{\rm eff}^{\rm in,out}(\Phi) \simeq V_{\rm eff}^{\rm in,out}(\Phi_{\rm min}^{\rm in,out}) + \frac{1}{2}\partial_{\Phi\Phi} V_{\rm eff}^{\rm in,out}(\Phi_{\rm min}^{\rm in,out})[\Phi - \Phi_{\rm min}^{\rm in,out}]^2, \tag{9}$$

and define the effective mass of the chameleon in the usual way:

$$m_{\rm eff}^{2\rm in,out}(\Phi_{\rm min}^{\rm in,out}, \beta_i, T_{\rm in,out}^m) = \partial_{\Phi\Phi} V_{\rm eff}^{\rm in,out}(\Phi_{\rm min}^{\rm in,out}). \tag{10}$$

In particular, setting $\beta_i = \beta$, the expression for the effective mass $m_{\rm eff}^{\rm in,out}$ turns out to be:

$$m_{\rm eff}^{2\rm in,out}(\Phi_{\rm min}^{\rm in,out}, \beta, T_{\rm in,out}^m) = \lambda n(n+1) M^2 \Big(\frac{M}{\Phi_{\rm min}^{\rm in,out}}\Big)^{n+2}, \tag{11}$$

with

$$\Phi_{\rm min}^{\rm in,out} = M\Big(\frac{n\lambda M_{pl} M^3}{-\beta T_{\rm in,out}^m}\Big)^{\frac{1}{n+1}}. \tag{12}$$

Expressions (11) and (12) are valid when n is a positive integer or a negative even integer, as otherwise a minimum does not exist. Furthermore, for $n = -2$ the effective mass of the chameleon does not depend on the composition of the *smaller* body, the *larger* body and/or the environment. This however does not mean that the model avoids predictions for violations of WEP. The value of the scalar field does depend, even if only very slightly, on the size and composition of the smaller body, and this would lead, in principle, to some dependence of the acceleration on the body's composition in actual tests. We face however a problem in attempting to estimate this quantity numerically, because, in contrast with other situations, in this case the estimate value for the cutoff N for the series would be of the order of a thousand, and thus a reliable calculation would require a more complex treatment which is beyond the scope of this manuscript.

A. Implementation of the Approach

Next, we perform the calculation of the chameleon in the presence of two bodies without, in principle, neglecting any contribution, but still in the *quasilinear* approximation discussed before[10]. The problem is depicted in Fig. 1

In order to do so, we expand the most general solution for the two body problem in complete sets of solutions of the differential equation in the inside and outside regions determined by the two bodies. Thus we write,

$$\Phi = \begin{cases} \Phi_{\rm in1} = \sum\limits_{lm} C_{lm}^{\rm in1} i_l(\mu_1 r) Y_{lm}(\theta,\phi) + \Phi_{\rm 1min}^{\rm in} & (r \le R_1) \\ \Phi_{\rm out} = \sum\limits_{lm} C_{lm}^{\rm out1} k_l(\mu_{\rm out} r) Y_{lm}(\theta,\phi) + C_{lm}^{\rm out2} k_l(\mu_{\rm out} r') Y_{lm}(\theta',\phi') + \Phi_\infty & \text{(exterior solution)} \\ \Phi_{\rm in2} = \sum\limits_{lm} C_{lm}^{\rm in2} i_l(\mu_2 r') Y_{lm}(\theta',\phi') + \Phi_{\rm 2min}^{\rm in} & (r' \le R_2) \end{cases} \tag{13}$$

where $\mu_1 = m_{\rm eff}^{\text{large body}}$, $\mu_{\rm out} = m_{\rm eff}^{\rm out}$, $\mu_2 = m_{\rm eff}^{\text{test body}}$ and R_1, R_2 are the radii of the larger and test bodies, respectively, and i_l and k_l are Modified Spherical Bessel Functions (MSBF). In the above equation, the coordinate system x,y,z is centered in the larger body, while the coordinate system x',y',z' is centered in the test body (see Fig. 1). Notice that in writing Eq. (13) we have taken into account the regularity conditions of the scalar field at the center of both bodies. That is, the MSBF used in the expansions for the solutions inside both bodies are well behaved within their corresponding compact supports. Conversely, for the exterior solution (i.e. the solution outside both bodies) we employ the set of MSBF functions associated with each body which are well behaved at infinity. Furthermore, the coefficients C_{lm} of Eq. (13) are calculated using the following continuity conditions for the field and its derivative at the boundaries of the two bodies:

$$\Phi_{\rm in1}(r = R_1) = \Phi_{\rm out}(r = R_1), \qquad \partial_r \Phi_{\rm in1}(r = R_1) = \partial_r \Phi_{\rm out}(r = R_1),$$

[10] The quasilinear approach can be improved by going to higher order perturbation theory. We will explore this explicitly in Appendix E

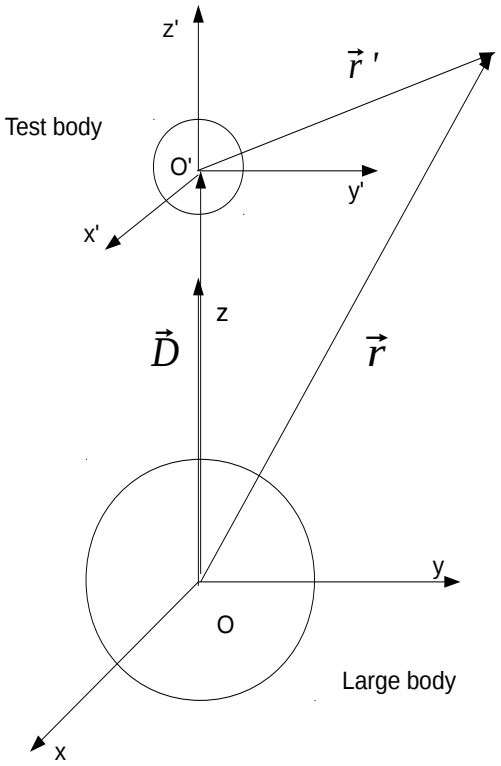

Figure 1: Two body problem.

$$\Phi_{\rm in2}(r'=R_2)=\Phi_{\rm out}(r'=R_2),\qquad \partial_{r'}\Phi_{\rm in2}(r'=R_2)=\partial_{r'}\Phi_{\rm out}(r'=R_2);$$

In order to describe properly the two body problem in a single coordinate system we can use the following relationship that links the special functions in the two coordinate systems [26, 30]:

$$k_l(\mu_{\rm out}r)Y_{lm}(\theta,\phi)=\sum_{vw}\alpha^{*lm}_{vw}i_v(\mu_{\rm out}r')Y_{vw}(\theta',\phi'), \tag{14}$$

where the coefficients α^{*lm}_{vw} can be expressed as follows:

$$\begin{aligned}\alpha^{*lm}_{vw}=&(-1)^{m+v}(2v+1)\sum_{p=|l-v|}^{|l+v|}(-1)^{-p}(2p+1)\Big[\frac{(l+m)!(v+w)!(p-m-w)!}{(l-m)!(v-w)!(p+m+w)!}\Big]^{1/2}\\ &\times\begin{bmatrix}l & v & p\\ 0 & 0 & 0\end{bmatrix}\begin{bmatrix}l & v & p\\ m & w & -m-w\end{bmatrix}k_p(\mu_{\rm out}|D|)Y_{p(m-w)}(\theta_D,\phi_D),\end{aligned} \tag{15}$$

being θ_D and ϕ_D the angular coordinates of $\vec{D}$ (see Fig. 1) and we remind the reader that D is the distance between the center of the two bodies. Moreover, we can use a similar relationship between the special functions given in terms of the coordinates centered in the test body with the ones centered in the larger body:

$$k_l(\mu_{\rm out}r')Y_{lm}(\theta',\phi')=\sum_{vw}\alpha^{lm}_{vw}i_v(\mu_{\rm out}r)Y_{vw}(\theta,\phi), \tag{16}$$

where

$$\begin{aligned}\alpha^{lm}_{vw}=&(-1)^{m+v}(2v+1)\sum_{p=|l-v|}^{|l+v|}(2p+1)\Big[\frac{(l+m)!(v+w)!(p-m-w)!}{(l-m)!(v-w)!(p+m+w)!}\Big]^{1/2}\\ &\times\begin{bmatrix}l & v & p\\ 0 & 0 & 0\end{bmatrix}\begin{bmatrix}l & v & p\\ m & w & -m-w\end{bmatrix}k_p(\mu_{\rm out}|D|)Y_{p(m-w)}(\theta_D,\phi_D),\end{aligned} \tag{17}$$

valid for $|r| \leq |D|$ and $|r'| \leq |D|$. We are still assuming axial symmetry around the $z-$axis, and the coordinate transformation is, in this case, a translation. Therefore, only the terms with $m = w = 0$ do contribute to the expansions. An approximate expression for the chameleon field is found by truncating the infinite series Eqs. (14) and (16). We further note that as shown in Refs.[24, 25], the series of this type can be estimated by truncating the sum after the first N terms, with N given by the integer part of $N_0 = \frac{e\mu_{\rm out}|D|}{2}$ where e is Euler's number. Using this last result we can solve the following two equations for $C_l^{\rm out1}$ and $C_l^{\rm out2}$; the first one reads:

$$b_1\delta_{l0} = C_l^{\rm out1}a_l + \sum_{w=0}^{N} C_w^{\rm out2} z_{wl}, \tag{18}$$

where

$$a_l = \frac{k_l'(\mu_{\rm out}R_1)i_l(\mu_1 R_1)}{i_l'(\mu_1 R_1)} - k_l(\mu_{\rm out}R_1), \tag{19}$$

$$z_{wl} = \alpha_{l0}^{w0}\Big[i_l(\mu_{\rm out}R_1) - \frac{i_l'(\mu_{\rm out}R_1)i_l(\mu_1 R_1)}{i_l'(\mu_1 R_1)}\Big], \tag{20}$$

$$b_1 = \sqrt{4\pi}(\Phi_\infty - \Phi_{\rm 1min}^{\rm in}). \tag{21}$$

where a *prime* ' ' indicates differentiation of the MSBF with respect to its argument.

The second equation reads:

$$b_2\delta_{l0} = C_l^{\rm out2}x_l + \sum_{w=0}^{N} C_w^{\rm out1} y_{wl}, \tag{22}$$

where

$$x_l = \frac{k_l'(\mu_{\rm out}R_2)i_l(\mu_2 R_2)}{i_l'(\mu_2 R_2)} - k_l(\mu_{\rm out}R_2), \tag{23}$$

$$y_{wl} = \alpha_{l0}^{*w0}\Big[i_l(\mu_{\rm out}R_2) - \frac{i_l'(\mu_{\rm out}R_2)i_l(\mu_2 R_2)}{i_l'(\mu_2 R_2)}\Big], \tag{24}$$

$$b_2 = \sqrt{4\pi}(\Phi_\infty - \Phi_{\rm 2min}^{\rm in}). \tag{25}$$

We can now write the system of equations for the coefficients $C_l^{\rm in1}$ and $C_l^{\rm in2}$ associated with the interior solutions in terms of the coefficients of the exterior solution:

$$C_l^{\rm in1}i_l'(\mu_1 R_1) = C_l^{\rm out1}k_l'(\mu_{\rm out}R_1) + \sum_{w=0}^{N} C_w^{\rm out2}\alpha_{l0}^{w0}i_l'(\mu_{\rm out}R_1), \tag{26}$$

$$C_l^{\rm in2}i_l'(\mu_2 R_2) = C_l^{\rm out2}k_l'(\mu_{\rm out}R_2) + \sum_{w=0}^{N} C_w^{\rm out1}\alpha_{l0}^{*w0}i_l'(\mu_{\rm out}R_2). \tag{27}$$

In this way, by solving the system of equations (18) and (22) we can obtain a solution of the two body problem for the chameleon where the only approximation (within the quasilinear approach) consists in the truncation of the series used for the transformation of coordinates. The dependence of the field on the composition of the test body appears through the constants $C_l^{\rm out1}$ and $C_l^{\rm out2}$.

Figure 2 depicts the field around the centers of the two bodies and outside them along the $z-$axis[11] which results from our method by cutting off the series expansions after taking the first three terms in each one[12], while Figure 3 shows the field near the surfaces. Note that under the conditions $1 \ll \mu_{1,2}R_{1,2}$, which are valid within each body, the thin-shell effect appears in both bodies. Namely, the field is almost constant with values close to $\Phi_{\rm min\,1,2}$ in each body, respectively, and grows exponentially near the surfaces. As expected, the *thin shell* effect is more pronounced

[11] In each case, the origin of $z-$axis is in the center of each body.

[12] The same result is obtained if only the first term of the series is used, as this turns out to be many orders of magnitude larger than the following terms.

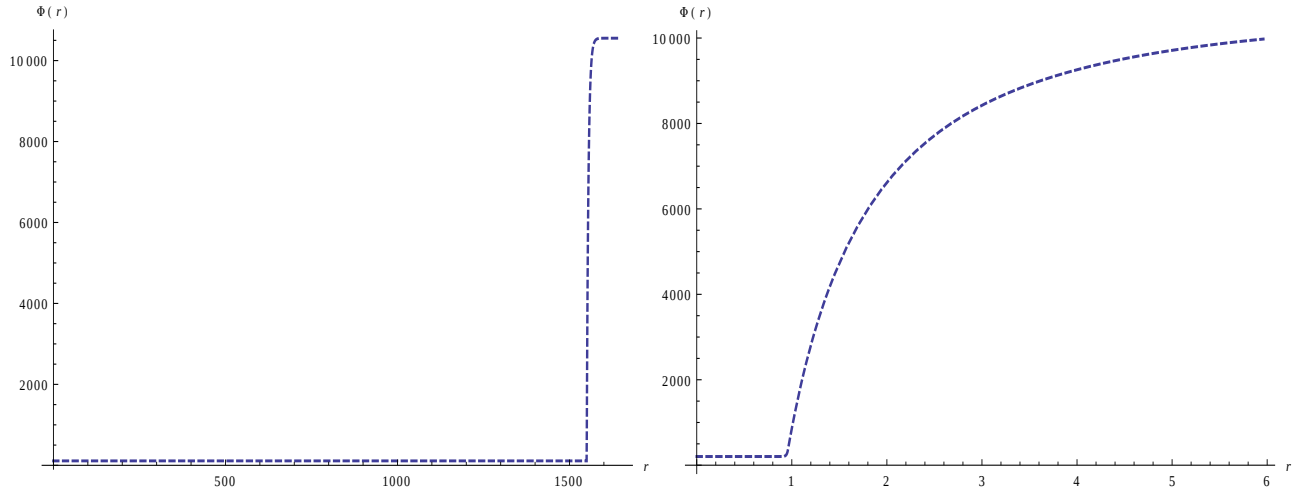

(a) Chameleon field within a neighborhood of the larger body (b) Chameleon field within a neighborhood of the test body

Figure 2: The chameleon field Φ as a function of coordinate r inside the bodies (including the centers at $r = 0$) and in their outskirts (r is the distance to the center of the body in cm, then Φ is measured in cm^{-1}). In each panel the r coordinate is taken from the center of each body for convenience. Panel (a): the larger body consists of a sphere of radius $R_1 = 1550$ cm and $\mu_1 = 197.2244\ \text{cm}^{-1}$. This body mimics roughly the actual hill where the experiment of the Eöt-Wash group takes place and which produces the desired combined effects (gravitational and "fifth" force if any). Panel (b): the test body (a 10 gr sphere of aluminum), $R_2 = 0.96$ cm and $\mu_2 = 78.1940\ \text{cm}^{-1}$. In both cases $n = 1 = \beta = 1$ and $M = 120.695\ \text{cm}^{-1}$.

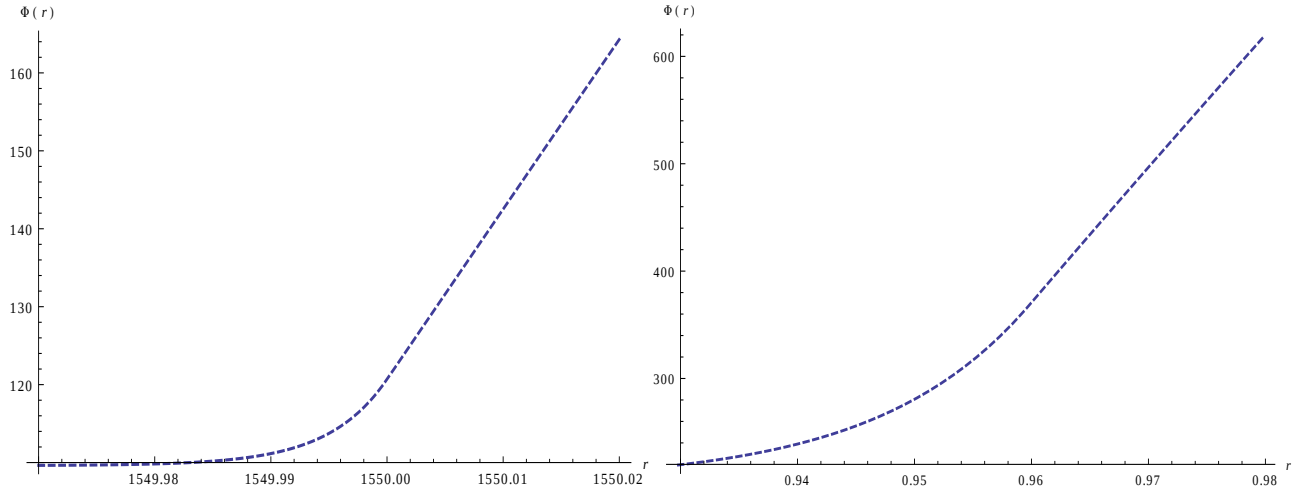

(a) Chameleon field near the surface of the larger body (b) Chameleon field near the surface of the test body

Figure 3: The chameleon field Φ as a function of coordinate r near the surfaces of the two bodies (r is the distance to the center of the body in cm). The parameters and the configuration of the bodies is the same as in Figure 2.

in the larger body (see Figure 3a) than in the test body (see Figure 3b) since $\mu_2 R_2 < \mu_1 R_1$. As μR becomes smaller, the *thin shell* disappears. Remarkably, despite the presence of thin-shells in both objects (but not relying on any further approximation based on a small value of $\frac{\Delta R}{R}$– see Appendix D), we find that the force between them is not suppressed to the level of avoiding the bounds imposed by the WEP experiments. We will analyze this in much more detail in the following section.

III. FORCE ON A FREE FALLING BODY AND VIOLATION OF THE WEP

In this section we calculate the force between the two bodies due to the scalar-field interaction and estimate the expected magnitude of the effective violation of WEP. This force, together with the gravitational force on the test body, will be considered as characterizing a "free falling" test body in laboratory conditions under the influence of both interactions.

We begin by finding an expression for this force from first principles, and then, we apply the formula for the two-body problem that we analyzed in the previous section. Later we compute the resulting Eötvös parameter associated with the acceleration of two test bodies.

We obtain the chameleon mediated force from the variation with distance of the interaction energy associated with this field. Clearly, this energy can be obtained from integrating the corresponding component of the EMT associated with the system, which in turn, is the source of the Einstein's field equations of the model. Thus, we focus on the gravitational field equations that are obtained from varying the action (1) with respect to $g^{\mu\nu}$: [13]

$$G_{\mu\nu} = \frac{1}{M_{pl}^2}\left(T^{\Phi}_{\mu\nu}+T^{m}_{\mu\nu}\right) \ , \tag{28}$$

$$T^{\Phi}_{\mu\nu} = (\nabla_\mu\Phi)(\nabla_\nu\Phi) - g_{\mu\nu}\left[\frac{1}{2}g^{\alpha\beta}(\nabla_\alpha\Phi)(\nabla_\beta\Phi)+V(\Phi)\right] \ , \tag{29}$$

where, as before, we assume $T^{m}_{\mu\nu}=u_\mu u_\nu(\rho+P)+g_{\mu\nu}P$ for the EMT of matter. Now the energy associated with the total EMT under the assumptions of staticity and flat spacetime is

$$\begin{aligned} U &= \int_V \left(T^{\Phi}_{00}+T^{m}_{00}\right)dV = \int_V\left[\frac{1}{2}(\nabla^i\Phi)(\nabla_i\Phi)+V(\Phi)+\rho\right]dV \\ &= \int_V\left[\frac{1}{2}(\nabla^i\Phi)(\nabla_i\Phi)+V_{\rm eff}(\Phi)+\rho+\frac{\beta\Phi T^m}{M_{pl}}\right]dV \ , \end{aligned} \tag{30}$$

where the time components of both EMT's are taken with respect to an observer that is static relative to the two-body configuration [14]. In the last line we used Eq. (9). The term containing the spatial gradients of the field can be integrated by parts:

$$U=\int_V\left[-\frac{1}{2}\Phi\nabla^2\Phi+V_{\rm eff}(\Phi)+\rho+\frac{\beta\Phi T^m}{M_{pl}}\right]dV=\int_V\left[-\frac{1}{2}\Phi\partial_\Phi V_{\rm eff}(\Phi)+V_{\rm eff}(\Phi)+\rho+\frac{\beta\Phi T^m}{M_{pl}}\right]dV \ , \tag{31}$$

where we discarded the surface term that arises from $\int_V\nabla_i(\Phi\nabla^i\Phi)dV$, and used Eq. (6) in the last step. Now, using Eq. (7) and (3) we obtain

$$U=\int_V\left[\frac{1}{2}V(\Phi)(2+n)+\frac{\beta\Phi T^m}{2M_{pl}}+\rho\right]dV=\int_V\left[\frac{1}{2}V_{\rm eff}(\Phi)(2+n)+\frac{(3+n)\beta\Phi T^m}{2M_{pl}}+\rho\right]dV \ . \tag{32}$$

We can write this equation as

$$U=\int_V\left[\frac{1}{2}V_{\rm eff}(\Phi)(2+n)+\frac{(3+n)\beta(\Phi-\Phi_{\rm min})T^m}{2M_{pl}}+\frac{(3+n)\beta\Phi_{\rm min}T^m}{2M_{pl}}+\rho\right]dV \ . \tag{33}$$

Taking Eq. (9) for the approximation of $V_{\rm eff}(\Phi)$ about its minimum, the above equation reduces to

$$U\approx\int_V\left[\frac{(2+n)}{4}m^2_{\rm eff}\hat{\Phi}^2+\frac{(3+n)\beta\hat{\Phi}T^m}{2M_{pl}}+\frac{(n+2)}{2}V_{\rm eff}(\Phi_{\rm min})+\frac{(3+n)\beta\Phi_{\rm min}T^m}{2M_{pl}}+\rho\right]dV \ . \tag{34}$$

---

[13] From the Bianchi identities followed by the use of Eq. (6) one can see that the EMT of matter is not conserved in the Einstein frame: $\nabla^\mu T^m_{\mu\nu}=T^m(\partial_\Phi \ln A)\nabla_\nu\Phi$,where $A^2=e^{2\beta\Phi/M_{pl}}$ is the conformal factor between the Einstein-frame metric and the geodesic metrics [cf. Eq. (2)].We then obtain $\nabla^\mu T^m_{\mu\nu}=T^m\beta/M_{pl}\nabla_\nu\Phi$. The right-hand side of this equation is precisely related with the chameleon force [cf. Eq. (C8)]

[14] That is, we take a reference frame defined by the unit time-like vector (4-velocity) $n^\mu=\left(\frac{\partial}{\partial t}\right)^\mu$ as to coincide with u^μ, such that $T^{\rm tot}_{00}=n^\mu n^\mu T^{\rm tot}_{\mu\nu}$, where $T^{\rm tot}_{\mu\nu}=T^{\Phi}_{\mu\nu}+T^{m}_{\mu\nu}$. The staticity assumption translates into $n^\mu\partial_\mu\Phi=0$.

where $\hat{\Phi} = \Phi - \Phi_{\rm min}$.

The only approximation we have made so far for the energy of the whole system is to replace the effective potential of the chameleon with the corresponding expansion around its minimum in each of the three regions (i.e. the two bodies and the environment) which is the usual procedure. The approximate effective potentials obtained from Eq. (9) do not deviate substantially from the corresponding *exact* potentials Eq. (7) as one can see in Figures 1 and 2 of Ref. [16].

We can now compute the chameleon mediated force using $F_{z\Phi} = -\frac{\partial U}{\partial D}$, where D is the distance between the center of the two bodies. To this aim, we first notice that the last three terms within the integral of Eq. (34) are independent of the separation D of the bodies, and thus, do not contribute to the force, i.e., $\frac{\partial}{\partial D}\{\int_V [\frac{(n+2)}{2} V_{\rm eff}(\Phi_{\rm min}) + \frac{(3+n)\beta\Phi_{\rm min})T^m}{2M_{pl}} + \rho] dV\} = 0$ [15].

In order to calculate the total energy, we have to consider the contributions due to the chameleon in the regions inside the two bodies and in the region exterior to both bodies. To do so, let us define V_1 as the region corresponding to the larger body, V_2 as the region corresponding to the test body, and V_3 is the region exterior to the larger body in the coordinate system centered in the larger body:

$$V_3 = \begin{cases} R_1 \leq r \leq \infty \\ 0 \leq \theta \leq \pi \\ 0 \leq \phi \leq 2\pi \end{cases} \tag{35}$$

Thus, the total energy can be written as:

$$\begin{aligned} U &= \int_{\text{large body}} t_{00}[\hat{\Phi}(V_1)] dV_1 + \int_{\text{test body}} t_{00}[\hat{\Phi}(V_2)] dV_2 + \int_{\text{outside bodies}} t_{00}[\hat{\Phi}(\text{out})] dV_{out} \\ &= \int_{V_1} t_{00}[\hat{\Phi}(V_1)] dV_1 + \int_{V_2} t_{00}[\hat{\Phi}(V_2)] dV_2 + \int_{V_3} t_{00}[\hat{\Phi}(\text{out})] dV_3 - \int_{V_2} t_{00}[\hat{\Phi}(\text{out})] dV_2 \end{aligned} \tag{36}$$

where $t_{00} = \frac{(2+n)}{4} m_{\rm eff}^2 \hat{\Phi}^2 + \frac{(3+n)\beta\hat{\Phi}T^m}{2M_{pl}}$ corresponds to the first two terms of Eq. (34) which are the responsible for the force between the two bodies. Here $\hat{\Phi}(\text{out})$ refers to the field outside the two bodies. This is why we have to subtract the last term. In consequence, the total force can be expressed as:

$$\begin{aligned} F_{z\Phi} &= \frac{\partial}{\partial D} \int_{V_2} \Big\{ \hat{\Phi}_{\rm in2}(\vec{r}\,') \Big[\frac{(n+3)}{2} \frac{\rho_2 \beta}{M_{pl}} \Big] - \frac{(2+n)\mu_2^2 \hat{\Phi}_{\rm in2}^2(\vec{r}\,')}{4} \Big\} d^3\vec{r}\,' \\ &+ \frac{\partial}{\partial D} \int_{V_1} \Big\{ \hat{\Phi}_{\rm in1}(\vec{r}) \Big[\frac{(n+3)}{2} \frac{\rho_1 \beta}{M_{pl}} \Big] - \frac{(2+n)\mu_1^2 \hat{\Phi}_{\rm in1}^2(\vec{r})}{4} \Big\} d^3\vec{r} \\ &+ \frac{\partial}{\partial D} \int_{V_3} \Big\{ \hat{\Phi}_{\rm out}(\vec{r}) \Big[\frac{(n+3)}{2} \frac{\rho_{\rm out} \beta}{M_{pl}} \Big] - \frac{(2+n)\mu_{\rm out}^2 \hat{\Phi}_{\rm out}^2(\vec{r})}{4} \Big\} d^3\vec{r} \\ &- \frac{\partial}{\partial D} \int_{V_2} \Big\{ \hat{\Phi}_{\rm out}(\vec{r}\,') \Big[\frac{(n+3)}{2} \frac{\rho_{\rm out} \beta}{M_{pl}} \Big] - \frac{(2+n)\mu_{\rm out}^2 \hat{\Phi}_{\rm out}^2(\vec{r}\,')}{4} \Big\} d^3\vec{r}\,'; \end{aligned} \tag{37}$$

where we used $T^m \approx -\rho$, and ρ_1 and ρ_2 are the densities of the larger and the test bodies, respectively, and $\rho_{\rm out}$ is the density of the *environment* (i.e. the density outside both bodies).

In the last two integrals of Eq. (37), we have to rewrite the chameleon in terms of the corresponding coordinates adapted to each body [24–26, 30]. Moreover, we neglect the contribution of the second part of $\hat{\Phi}_{\rm out}$ given by $\sum_{lm} C_{lm}^{\rm out2} k_l(\mu_{\rm out} r') Y_{lm}(\theta', \phi')$, to the last integral [i.e. we take $\hat{\Phi}_{\rm out}(\vec{r}\,') \approx \sum_{lm} C_{lm}^{\rm out1} \sum_{w=0}^{N} \alpha_{w0}^{*l0} i_w(\mu_{\rm out} r') Y_{w0}(\theta', \phi')$] because that contribution is negligible in comparison with the other one.

Each integral of the above equation has a linear term in Φ and a squared term (Φ^2). Therefore, we separate $F_{z\Phi}$ in two terms, a linear one $F_{1z\Phi}$ and a squared one $F_{2z\Phi}$ such that $F_{z\Phi} = F_{1z\Phi} + F_{2z\Phi}$. Then,

---

[15] As usual, the integral $\int_V V_{\rm eff}(\Phi_{\rm min}) dV$ (in all the space) is an infinite constant.

$$
\begin{aligned}
F_{1z\Phi} \;=\; & \int_0^{R_2}\int_0^{\pi}\int_0^{2\pi}\Big[\frac{(n+3)}{2}\frac{\rho_2\beta}{M_{pl}}\Big]\Big[\sum_l \frac{\partial C_{l0}^{\rm in2}}{\partial D} i_l(\mu_2 r')Y_{l0}(\theta',\phi')\Big] r'^2\sin(\theta')d\phi' d\theta' dr' \\
+ & \int_0^{R_1}\int_0^{\pi}\int_0^{2\pi}\Big[\frac{(n+3)}{2}\frac{\rho_1\beta}{M_{pl}}\Big]\Big[\sum_l \frac{\partial C_{l0}^{\rm in1}}{\partial D} i_l(\mu_1 r)Y_{l0}(\theta,\phi)\Big] r^2\sin(\theta)d\phi d\theta dr \\
+ & \int_{R_1}^{\infty}\int_0^{\pi}\int_0^{2\pi}\Big[\frac{(n+3)}{2}\frac{\rho_{\rm out}\beta}{M_{pl}}\Big]\Big[\sum_l \frac{\partial C_{l0}^{\rm out1}}{\partial D} k_l(\mu_{\rm out} r)Y_{l0}(\theta,\phi)\Big] r^2\sin(\theta)d\phi d\theta dr \\
+ & \int_{R_1}^{D}\int_0^{\pi}\int_0^{2\pi}\Big[\frac{(n+3)}{2}\frac{\rho_{\rm out}\beta}{M_{pl}}\Big] \\
\times & \Big[\sum_l\sum_{w=0}^{N}\Big\{\frac{\partial C_{l0}^{\rm out2}}{\partial D}\alpha_{w0}^{l0} + C_{l0}^{\rm out2}\frac{\partial \alpha_{w0}^{l0}}{\partial D}\Big\} i_w(\mu_{\rm out} r)Y_{w0}(\theta,\phi)\Big] r^2\sin(\theta)d\phi d\theta dr \\
+ & \int_{D}^{\infty}\int_0^{\pi}\int_0^{2\pi}\Big[\frac{(n+3)}{2}\frac{\rho_{\rm out}\beta}{M_{pl}}\Big] \\
\times & \Big[\sum_l\sum_{w=0}^{N}\Big\{\frac{\partial C_{l0}^{\rm out2}}{\partial D}\hat{\alpha}_{w0}^{l0} + C_{l0}^{\rm out2}\frac{\partial \hat{\alpha}_{w0}^{l0}}{\partial D}\Big\} k_w(\mu_{\rm out} r)Y_{w0}(\theta,\phi)\Big] r^2\sin(\theta)d\phi d\theta dr \\
- & \int_0^{R_2}\int_0^{\pi}\int_0^{2\pi}\Big[\frac{(n+3)}{2}\frac{\rho_{\rm out}\beta}{M_{pl}}\Big] \\
\times & \Big[\sum_l\sum_{w=0}^{N}\Big\{\frac{\partial C_{l0}^{\rm out1}}{\partial D}\alpha_{w0}^{*l0} + C_{l0}^{\rm out1}\frac{\partial \alpha_{w0}^{*l0}}{\partial D}\Big\} i_w(\mu_{\rm out} r')Y_{w0}(\theta',\phi')\Big] r'^2\sin(\theta')d\phi' d\theta' dr',
\end{aligned}
\tag{38}
$$

where

$$
\begin{aligned}
\hat{\alpha}_{vw}^{lm} =& (-1)^{m+v}(2v+1)\sum_{p=|l-v|}^{|l+v|}(2p+1)\Big[\frac{(l+m)!(v+w)!(p-m-w)!}{(l-m)!(v-w)!(p+m+w)!}\Big]^{1/2} \\
& \times \begin{bmatrix} l & v & p \\ 0 & 0 & 0 \end{bmatrix}\begin{bmatrix} l & v & p \\ m & w & -m-w \end{bmatrix} i_p(\mu_{\rm out}|D|)Y_{p(m-w)}(\theta_D,\phi_D).
\end{aligned}
\tag{39}
$$

The integral $\int_0^{2\pi}\int_0^{\pi} Y_{l0}(\theta_j,\phi_j)\sin(\theta_j)d\theta_j d\phi_j$, which appears inside all the terms in the expression for $F_{1z\Phi}$, vanishes when $l \neq 0$. Meanwhile, integrals like $\int_0^R i_l(mr)r^2dr$ and $\int_R^{\infty} k_l(mr)r^2dr$, and the derivatives $\partial C_{l0}^{\rm in(out)\,1(2)}/\partial D$ converge to finite values for all values of l. Consequently, the only contribution to the first three integrals of Eq. (38) is the term with $l = 0$, while the last integrals of Eq. (38) only have no null terms for $w = 0$ being l arbitrary in this

case. In this way, we obtain for the linear term of the force:

$$
\begin{aligned}
F_{1z\Phi} &= \Big[\frac{(n+3)}{2}\frac{\rho_2\beta}{M_{pl}}\Big]2\sqrt{\pi}\frac{\partial C_{00}^{\rm in2}}{\partial D}\Big[\frac{\mu_2 R_2\cosh(\mu_2 R_2)-\sinh(\mu_2 R_2)}{\mu_2^3}\Big] \\
&+ \Big[\frac{(n+3)}{2}\frac{\rho_1\beta}{M_{pl}}\Big]2\sqrt{\pi}\Big[\frac{\mu_1 R_1\cosh(\mu_1 R_1)-\sinh(\mu_1 R_1)}{\mu_1^3}\Big]\frac{\partial C_{00}^{\rm in1}}{\partial D} \\
&+ \Big[\frac{(n+3)}{2}\frac{\rho_{\rm out}\beta}{M_{pl}}\Big]2\sqrt{\pi}\frac{\partial C_{00}^{\rm out1}}{\partial D}\Big[\frac{\exp[-\mu_{\rm out}R_1](1+R_1)}{\mu_{\rm out}^3}\Big] \\
&+ \Big[\frac{(n+3)}{2}\frac{\rho_{\rm out}\beta}{M_{pl}}\Big]2\sqrt{\pi}\sum_l\Big\{\frac{\partial C_{l0}^{\rm out2}}{\partial D}\alpha_{00}^{l0}+C_{l0}^{\rm out2}\frac{\partial\alpha_{00}^{l0}}{\partial D}\Big\} \\
&\times \Big[\frac{-R_1\cosh(\mu_{\rm out}R_1)+D\cosh(\mu_{\rm out}D)}{\mu_{\rm out}^2}+\frac{\sinh(\mu_{\rm out}R_1)-\sinh(\mu_{\rm out}D)}{\mu_{\rm out}^3}\Big] \\
&+ \Big[\frac{(n+3)}{2}\frac{\rho_{\rm out}\beta}{M_{pl}}\Big]2\sqrt{\pi}\sum_l\Big\{\frac{\partial C_{l0}^{\rm out2}}{\partial D}\hat{\alpha}_{00}^{l0}+\frac{\partial\hat{\alpha}_{00}^{l0}}{\partial D}C_{l0}^{\rm out2}\Big\}\frac{\exp[-\mu_{\rm out}R_1](1+\mu_{\rm out}R_1)}{\mu_{\rm out}^3} \\
&- \Big[\frac{(n+3)}{2}\frac{\rho_{\rm out}\beta}{M_{pl}}\Big]2\sqrt{\pi} \\
&\times \sum_l\Big\{\frac{\partial C_{l0}^{\rm out1}}{\partial D}\alpha_{00}^{*l0}+\frac{\partial\alpha_{00}^{*l0}}{\partial D}C_{l0}^{\rm out1}\Big\}\Big[\frac{\mu_{\rm out}R_2\cosh(\mu_{\rm out}R_2)-\sinh(\mu_{\rm out}R_2)}{\mu_{\rm out}^3}\Big].
\end{aligned}
\tag{40}
$$

The quadratic term can be expressed as:

$$
\begin{aligned}
F_{2z\Phi} &= -\int_{V_2}\Big[\frac{(n+2)}{4}\mu_2^2\Big]\frac{\partial}{\partial D}\Big[\sum_w\sum_l C_{l0}^{\text{in2}} i_l(\mu_2 r')Y_{l0}(\theta',\phi')C_{w0}^{\text{in2}} i_w(\mu_2 r')Y_{w0}(\theta',\phi')\Big]r'^2\sin(\theta')dV_2 \\
&- \int_{V_1}\Big[\frac{(n+2)}{4}\mu_1^2\Big]\frac{\partial}{\partial D}\Big[\sum_w\sum_l C_{l0}^{\text{in1}} i_l(\mu_1 r)Y_{l0}(\theta,\phi)C_{w0}^{\text{in1}} i_l(\mu_1 r)Y_{w0}(\theta,\phi)\Big]r^2\sin(\theta)dV_1 \\
&- \int_{R_1}^{\infty}\int_0^{\pi}\int_0^{2\pi}\Big[\frac{(n+2)}{4}\mu_{\text{out}}^2\Big]\frac{\partial}{\partial D}\Big[\sum_v\sum_l C_{l0}^{\text{out1}} k_l(\mu_{\text{out}} r)Y_{l0}(\theta,\phi)C_{v0}^{\text{out1}} k_v(\mu_{\text{out}} r)Y_{v0}(\theta,\phi)\Big]r^2\sin(\theta)d\phi d\theta dr \\
&- \int_{R_1}^{D}\int_0^{\pi}\int_0^{2\pi}\Big[\frac{(n+2)}{4}\mu_{\text{out}}^2\Big] \\
&\times \frac{\partial}{\partial D}\Big[\sum_v\sum_l C_{l0}^{\text{out1}} k_l(\mu_{\text{out}} r)Y_{l0}(\theta,\phi)C_{v0}^{\text{out2}}\sum_w^N \alpha_{w0}^{v0} i_w(\mu_{\text{out}} r)Y_{w0}(\theta,\phi)\Big]r^2\sin(\theta)d\phi d\theta dr \\
&- \int_{D}^{\infty}\int_0^{\pi}\int_0^{2\pi}\Big[\frac{(n+2)}{4}\mu_{\text{out}}^2\Big] \\
&\times \frac{\partial}{\partial D}\Big[\sum_v\sum_l C_{l0}^{\text{out1}} k_l(\mu_{\text{out}} r)Y_{l0}(\theta,\phi)C_{v0}^{\text{out2}}\sum_w^N \hat{\alpha}_{w0}^{v0} k_w(\mu_{\text{out}} r)Y_{w0}(\theta,\phi)\Big]r^2\sin(\theta)d\phi d\theta dr \\
&- \int_{R_1}^{D}\int_0^{\pi}\int_0^{2\pi}\Big[\frac{(n+2)}{4}\mu_{\text{out}}^2\Big] \\
&\times \frac{\partial}{\partial D}\Big[\sum_l C_{l0}^{\text{out2}}\sum_u^N \alpha_{u0}^{l0} i_u(\mu_{\text{out}} r)Y_{u0}(\theta,\phi)\sum_v C_{v0}^{\text{out2}}\sum_w^N \alpha_{w0}^{v0} i_w(\mu_{\text{out}} r)Y_{w0}(\theta,\phi)\Big]r^2\sin(\theta)d\phi d\theta dr \\
&- \int_{D}^{\infty}\int_0^{\pi}\int_0^{2\pi}\Big[\frac{(n+2)}{4}\mu_{\text{out}}^2\Big] \\
&\times \frac{\partial}{\partial D}\Big[\sum_l C_{l0}^{\text{out2}}\sum_u^N \hat{\alpha}_{u0}^{l0} k_u(\mu_{\text{out}} r)Y_{u0}(\theta,\phi)\sum_v C_{v0}^{\text{out2}}\sum_w^N \hat{\alpha}_{w0}^{v0} k_w(\mu_{\text{out}} r)Y_{w0}(\theta,\phi)\Big]r^2\sin(\theta)d\phi d\theta dr \\
&+ \int_0^{R_2}\int_0^{\pi}\int_0^{2\pi}\Big[\frac{(n+2)}{4}\mu_{\text{out}}^2\Big] \\
&\times \frac{\partial}{\partial D}\Big[\sum_l C_{l0}^{\text{out1}}\sum_u^N \alpha_{u0}^{*l0} i_u(\mu_{\text{out}} r')Y_{u0}(\theta',\phi')\sum_v C_{v0}^{\text{out1}}\sum_w^N \alpha_{w0}^{*v0} i_w(\mu_{\text{out}} r')Y_{w0}(\theta',\phi')\Big]r^2\sin(\theta')d\phi' d\theta' dr'
\end{aligned}
\tag{41}
$$

The angular integral that appears inside all the terms in the expression for $F_{2z\Phi}$ is,

$$
\int_0^{2\pi}\int_0^{\pi} Y_{l0}(\theta_j,\phi_j)Y_{k0}(\theta_j,\phi_j)\sin(\theta_j)d\theta_j d\phi_j = \frac{4\pi\sqrt{(2l+1)(2k+1)}k!}{4\pi(2k+1)k!}\delta_{kl} = \delta_{kl}.
$$

Therefore,

$$
\begin{aligned}
F_{2z\Phi} &= -\sum_l \frac{(n+2)}{4}\mu_2^2\frac{\partial}{\partial D}\Big[C_{l0}^{\rm in2}C_{l0}^{\rm in2}\Big]\frac{R_2^3}{2}\Big\{\,[i_l(\mu_2R_2)]^2 - i_{l-1}(\mu_2R_2)i_{l+1}(\mu_2R_2)\Big\} \\
&- \sum_l \frac{(n+2)}{4}\mu_1^2\frac{\partial}{\partial D}\Big[C_{l0}^{\rm in1}C_{l0}^{\rm in1}\Big]\frac{R_1^3}{2}\Big\{\,[i_l(\mu_1R_1)]^2 - i_{l-1}(\mu_1R_1)i_{l+1}(\mu_1R_1)\Big\} \\
&- \sum_l \frac{(n+2)}{4}\mu_{\rm out}^2\frac{\partial}{\partial D}\Big[C_{l0}^{\rm out1}C_{l0}^{\rm out1}\Big]\frac{R_1^3}{2}\Big\{\,[k_l(\mu_{\rm out}R_1)]^2 - k_{l-1}(\mu_{\rm out}R_1)k_{l+1}(\mu_{\rm out}R_1)\Big\} \\
&- \sum_w\sum_l^N \frac{(n+2)}{4}\mu_{\rm out}^2\frac{\partial}{\partial D}\Big[C_{w0}^{\rm out2}C_{l0}^{\rm out1}\alpha_{l0}^{w0}\Big]\Big\{Q_2(l,D) - Q_2(l,R_1)\Big\} \\
&- \sum_w\sum_l^N \frac{(n+2)}{4}\mu_{\rm out}^2\frac{\partial}{\partial D}\Big[C_{w0}^{\rm out2}C_{l0}^{\rm out1}\hat{\alpha}_{l0}^{w0}\Big]\frac{D^3}{2}\Big\{\,[k_l(\mu_{\rm out}D)]^2 - k_{l-1}(\mu_{\rm out}D)k_{l+1}(\mu_{\rm out}D)\Big\} \\
&- \sum_l\sum_w\sum_v^N \frac{(n+2)}{4}\mu_{\rm out}^2\frac{\partial}{\partial D}\Big[C_{w0}^{\rm out2}C_{l0}^{\rm out2}\alpha_{v0}^{w0}\alpha_{v0}^{l0}\Big]\Big\{Q_3(v,D) - Q_3(v,R_1)\Big\} \\
&- \sum_w\sum_l\sum_v^N \frac{(n+2)}{4}\mu_{\rm out}^2\frac{\partial}{\partial D}\Big[C_{w0}^{\rm out2}C_{l0}^{\rm out2}\hat{\alpha}_{v0}^{w0}\hat{\alpha}_{v0}^{l0}\Big] \\
&\times \frac{D^3}{2}\Big\{\,[k_v(\mu_{\rm out}D)]^2 - k_{v-1}(\mu_{\rm out}D)k_{v+1}(\mu_{\rm out}D)\Big\} \\
&+ \sum_w\sum_l\sum_v^N \frac{(n+2)}{4}\mu_{\rm out}^2\frac{\partial}{\partial D}\Big[C_{w0}^{\rm out1}C_{l0}^{\rm out1}\alpha_{v0}^{*w0}\alpha_{v0}^{*l0}\Big] \\
&\times \frac{R_2^3}{2}\Big\{\,[i_v(\mu_{\rm out}R_2)]^2 - i_{v-1}(\mu_{\rm out}R_2)i_{v+1}(\mu_{\rm out}R_2)\Big\}\ , \qquad (42)
\end{aligned}
$$

where

$$
Q_2(l,r) = -\frac{2l+1}{4\mu_{\rm out}^3} + \frac{r^3}{2}\Big\{i_l(\mu_{\rm out}r)k_l(\mu_{\rm out}r) + i_{l-1}(\mu_{\rm out}r)k_{l-1}(\mu_{\rm out}r)\Big\},
$$

$$
Q_3(v,r) = \frac{r^3}{2}\Big\{\Big[i_v(\mu_{\rm out}r)\Big]^2 - i_{v-1}(\mu_{\rm out}r)i_{v+1}(\mu_{\rm out}r)\Big\}.
$$

The expressions for $F_{1z\Phi}$ and $F_{2z\Phi}$ show, the explicit dependence of the chameleon mediated force with the composition and size of the test body through the quantities ρ_2, $C_{l0}^{\rm in2}$, $C_{l0}^{\rm in1}$, $C_{l0}^{\rm out2}$, $C_{l0}^{\rm out1}$ and their derivatives.

IV. RESULTS

So far, we have found the analytical expressions for the force. We now proceed to the quantitative estimates for the predicted violation of WEP in a relevant experiment. We can compare the predictions of Eq. (37) with the experimental bounds on the differential acceleration of two bodies of different composition: $\eta \sim 2\frac{|\vec{a_1}-\vec{a_2}|}{|\vec{a_1}+\vec{a_2}|}$, where $\vec{a_i} = \vec{a}_{i\Phi} + \vec{g}$ $(i = 1, 2)$ is the acceleration of the $i-$test body due to the chameleon force $\vec{a}_{i\Phi}$, and the force of gravity $\vec{g}$, which is basically due to the gravitational field produced by the larger body.

In all the cases that we have analyzed we find that, although the quadratic terms of the chameleon field in the expression of the total energy (and hence the force) are the largest contributors, the linear terms cannot be ignored. In most cases, the "optimal " cutoff N in the series expansion, estimated as the integer part of N_0 turns out to be zero (cf. Section II A). Thus, we keep only the first term of each sum so as to avoid numerical instabilities. The value of N increases with increasing n and β, the effect being more pronounced for dependence on n. Furthermore, the value of N also increases with the density of the outside medium ρ_{out}. Therefore in some cases, the value of N is so large that it effectively impedes the calculation.

Moreover, regarding the summations over the infinite ranges for l and w in the series of Eq. (42) we have checked the rate of convergence and found that one obtains basically the same result when cutting off the sums at $w = 4$ and $l = 4$ than when taking only the dominant terms $l = 0$ and $w = 0$ (the relative difference between both calculations in the predicted value of the Eötvös parameter η is of order 5×10^{-3}) . The reason for this is that when l increases, k_l also increases but i_l decreases very rapidly. The main point is that the quantity C_l decreases faster with l than the corresponding rate of growth of k_l. In Appendix B we show, that the results obtained for $N = 4$ and taking the summations up to $l = 4$, are the same as those presented in this section. We have been able to perform calculations up to N = 20 and we have observed that the first terms, those corresponding to $l = w = 0$ are the ones representing the main contributions to the results.

On the other hand, in the Appendix C we study the test-particle limit by taking $R_2 \to 0$ as ρ_2 is kept constant, and see how the violations of the WEP in the Eötvös parameter are suppressed by the presence of a thin shell. In particular, this occurs even when the coupling is *not* universal.

One of the most stringent bounds regarding the possible violations of the WEP is found when comparing the differential acceleration of two test bodies (e.g. two test-balls of Beryllium and Aluminum) using the Earth or its local inhomogeneities, as the source of the acceleration; the experimental value is $\Delta a_{\rm Be-Al} = (-2.5 \pm 2.5) \times 10^{-15} {\rm m/s}^2$ [6]. These bounds are found with an extremely accurate instrument (known as the Eöt–Wash experiment) consisting of a continuously rotating torsion balance which measures the acceleration difference of test bodies with different composition. As discussed in Refs. [6] and [31], there are two sources for the relevant signals in short-range effects: a hillside of 28 m located close to the laboratory, and a layer of cement blocks added to the wall of the laboratory of 1.5 m (we estimate 1 m distance between the wall and the device). We model the short range sources by spherical masses at a given distance and consider only the contribution of the hillside, such as in Ref. [32]. For such a configuration, the differential acceleration on two test bodies due to the hill produces an Eötvös parameter $\eta^{\rm hill}_{\rm Be-Al} = (-3.61 \pm 3.47) \times 10^{-11}$. In order to characterize such a configuration in our expression for the force, we make the following assumption for the test bodies: for the masses we take $m_{\rm Be} = m_{\rm Al} \approx 10$ g and for the densities $\rho_{\rm Be} \simeq 1.85 {\rm g\ cm}^{-3}$, $\rho_{\rm Al} \simeq 2.70 {\rm g\ cm}^{-3}$, and $\rho_{\rm hill} \simeq 9.27 {\rm g\ cm}^{-3}$. We consider the bodies as surrounded by an environment of constant density $\rho_{\rm out}$ for we considered two values (so that people might, compare actual and possible experiments): i) the density of the vacuum chamber $\rho_{\rm out} = 10^{-7} {\rm g\ cm}^{-3}$; ii) the density of the Earth's atmosphere $\rho_{\rm out} = 10^{-3} {\rm g\ cm}^{-3}$ [16]. In addition, we consider for the mass M that appears in the chameleon potential the value [cf. Eq. (3)] $M = 120.7\ {\rm cm}^{-1}$ (equivalent to ~ 2.4 meV) which corresponds to the case where the chameleon's energy density is responsible for the current acceleration of the cosmic expansion. Moreover, we consider β within a range of values that ensure the existence of a thin shell in one or in the two bodies. For instance, if $\beta \geq 0.1$ a thin shell exists in both bodies. Figure 4 shows the predictions for the violations of the WEP taking $1 \leq n \leq 4$ and $10^{-5} \leq \beta \leq 10^3$ and considering the two different values for the density of the environment mentioned above [17]. In all the cases η decreases as n increases. Furthermore for $\beta < 1$ the computed value of η increases as β increases, while for $\beta > 1$ there is a small decrease of η as β increases. It is interesting to compare the effect of the density of the environment on the predicted values of η: for a fixed value of n and β when the density of the environment increases by several orders of magnitude, the value of η decreases several orders of magnitude so that for the case i) almost all cases considered, predict violation of bounds set by tests of the WEP, while for case ii) only for $n > 1$ and $\beta < 10^{-3}$ bounds set by tests of the WEP are not defied. We have also calculated the predicted violation of bounds set by tests of the WEP for $n < 0$ and $10^{-5} < \beta < 10^{-1.5}$ and the results are shown in Fig. 5[18] of η for $\beta > 10^{-1.5}$. We found that for these cases the model predicts no violation of bounds set by tests of the WEP.

Table I shows η for $\beta = 1/\sqrt{6}$, a value commonly used in $F(R)$ theories [33] considering the density of the environment equal to the vacuum's chamber's density. In all cases considered here, the bounds resulting from tests of the WEP are violated. On the other hand, we were unable to calculate η for $n < 0$ and $\beta = 1/\sqrt{6}$ due the large value of N.

Fig. 6 shows the prediction for violation of bounds set by tests of the WEP, where the effect of the metal encasing is included as a Yukawa-like suppression. To include the effects of the metal encasing on the two body problem

---

[16] We are assuming that the bodies are surrounded by an environment of constant density and located inside a vacuum chamber of approximately 1 m long. A more realistic model would be one that includes both, the Earth's atmosphere surrounding the large body (the hill), and the vacuum chamber's medium surrounding the test body, which in turn, is encased within a very thin layer representing the metal of the vacuum chamber.

[17] In the latter case and for $\beta > 1$ we were unable to estimate the effective violation of the WEP because, in this case the value of N (the cutoff in the series expansion used in relating the two coordinate systems) becomes very large . The same problem arises for the case $n < 0$ and $\beta > 10^{-1.5}$

[18] As in the case where the environment corresponds to the Earth's atmosphere and for $n > 0$, the very large value of N impedes the calculation

Table I: Differences in acceleration between Be-Al bodies with the chamber's atmosphere

M	$\eta_{\rm n=1}$	$\eta_{\rm n=2}$	$\eta_{\rm n=3}$	$\eta_{\rm n=4}$
(1)	(2)	(3)	(4)	(5)
120.695	1.26×10^{-5}	4.47×10^{-8}	2.82×10^{-9}	6.31×10^{-10}

Notes.- Columns: (1) value of the parameter M in cm^{-1}, (2), (3), (4) and (5) differences in acceleration between Be and Al bodies for $n=1,2,3,4$ respectively. The Eötvös parameter η is tabulated for a fixed value of $\beta=1/\sqrt{6}$.

calculated in section III, we have multiplied the value of η by a factor obtained by Upadhye [35] as follows:

$$\eta_Y = \mathrm{sech}(2m_{\rm shell}d)\eta \tag{43}$$

Here η_Y refers to the value of η where the Yukawa-like suppression is included, $m^2_{\rm shell}=\frac{n(n+1)M^{n+4}}{\phi^{n+2}_{\rm shell}}$ and $\phi_{\rm shell}=\frac{nM^{4+n}M_{pl}}{\beta\rho^{1/(n+1)}_{\rm shell}}$. In particular we used the values $d=1$ cm and $\rho_{\rm shell}=10$ g cm^{-3}. Let us recall than in the above mentioned work [35], both the large and the test body, and the metal shell around the test body are modeled by planar slabs while the environments are similarly modeled by planar gaps. The Yukawa-like suppression factor was obtained fitting numerical results to an analytical function. It should be noted that this is an approximation to the calculation and a more accurate estimation should be obtained by considering the joint effects of the large body, test body and metal shell. However, the mathematical complications of such calculations are beyond the scope of the present work. Furthermore, in the estimates we have done we have used an idealized a spherical symmetric geometry for the experimental device and we know that this does not reflect the actual situation in the laboratory. Thus, we must keep in mind, that the present estimation is missing the effect of any asymmetry in the experimental setup. It follows from the comparison of Fig. 4 and Fig. 6 that for $\beta>10^{-2}$ the intensity of the suppression is so important that it predicts no violation of bounds set by tests of the WEP. However it is important to stress that the above estimation is just a rough estimation and consideration of any asymmetry of the experimental device might change the results in a drastic manner.

Another setting that serves to test the WEP is the Lunar Laser Ranging (LLR) which, since 1969, has provided high-precision measurements of the Earth-Moon distance [39]. Reflectors placed on the lunar surface, allow the measurement of the round-trip travel time of short pulses of laser light, and thus to set limits on the differential acceleration of the Earth-Moon system in free fall towards the Sun. Figure 7 shows the violations of the bounds from tests of WEP based on the Lunar Laser Ranging experiment; for this we consider the Sun as the large body ($\rho_{SUN}=1.43$ g cm^{-3}, $R_{SUN}=7\times10^8$ m) and the Earth and the Moon as test bodies: $\rho_E=5.5$ g cm^{-3}, $R_E=6.371\times10^6$ m, $\rho_M=3.34$ g cm^{-3}, $R_M=1.737\times10^6$ m. We consider two scenarios for the environment of the bodies: i) all bodies are surrounded by an environment of constant density equal to the density of the interstellar medium; ii) Earth and Sun surrounded by two regions of constant density $\rho_{\rm out1}$ equal to the Earth's or Sun's own atmosphere and $\rho_{\rm out2}=\rho_{\rm interstellar}$ while the Moon is surrounded by the interstellar medium. It follows from Fig. 7 that the bounds from tests of the WEP are violated only for $n=1$ and $\beta<10$ in case i) and in case ii) only for $n=1$ and $\beta<10^{-1}$. The prediction of η for the LLR in the case $\beta=1/\sqrt{6}$ is shown in Tables II and III. In the scenario i) and with the exception of the important case corresponding to $n=1$, the bounds from tests of the WEP are not violated.

In summary, in this section we have analyzed the predictions of the effective violation of the WEP that would result from the chameleon mediated forces in the model considering two different possibilities for the outside medium, by using Eqs. (40) and (42), and compared our results with the experimental bounds. Furthermore, when adding the effect of the vacuum's chamber metal encasing as a Yukawa-like suppression, results change significantly with respect to the estimates that ignore it, and the new prediction involves no violation of bounds set by tests of the WEP for $\beta>10^{-2}$. On the other hand, we also considered the LLR experiment, where there is no such suppression; in this case, one predicts violation of bounds set by tests of the WEP for $n=1$ and $\beta>10^{-1}$.

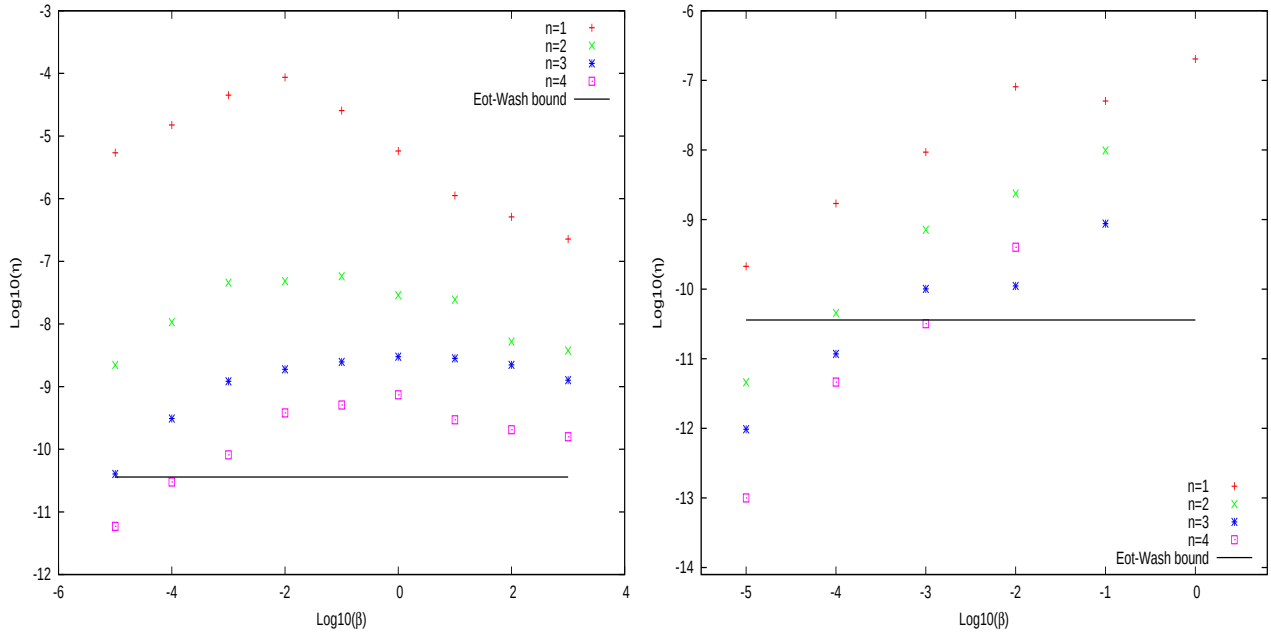

(a) η results for $\rho_{\rm out} = 10^{-7}$g cm^{-3}

(b) η results for $\rho_{\rm out} = 10^{-3}$g cm^{-3}

Figure 4: The Eötvös parameter η (in $\log_{10}$ scale) as a function of the parameter β (in $\log_{10}$ scale) for different positive values of n. The density of the environment $\rho_{\rm out}$ is assumed to be equal to: Panel (a) the vacuum's density inside the vacuum chamber $\rho_{\rm out} = 10^{-7}$g cm^{-3}; Panel (b) the Earth's atmosphere density $\rho_{\rm out} = 10^{-3}$g cm^{-3}

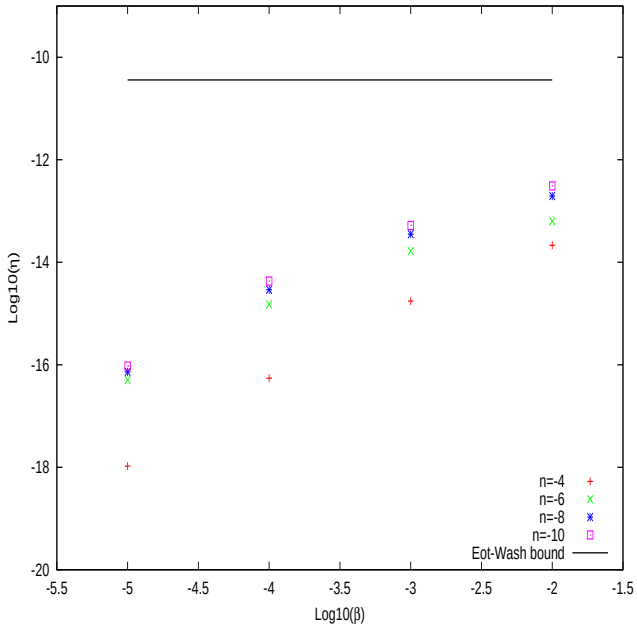

Figure 5: The Eötvös parameter η (in $\log_{10}$ scale) as a function of the parameter β (in $\log_{10}$ scale) for different negative values of n. The density of the environment $\rho_{\rm out}$ is assumed to be equal to the vacuum's density inside the vacuum chamber $\rho_{\rm out} = 10^{-7}$g cm^{-3}

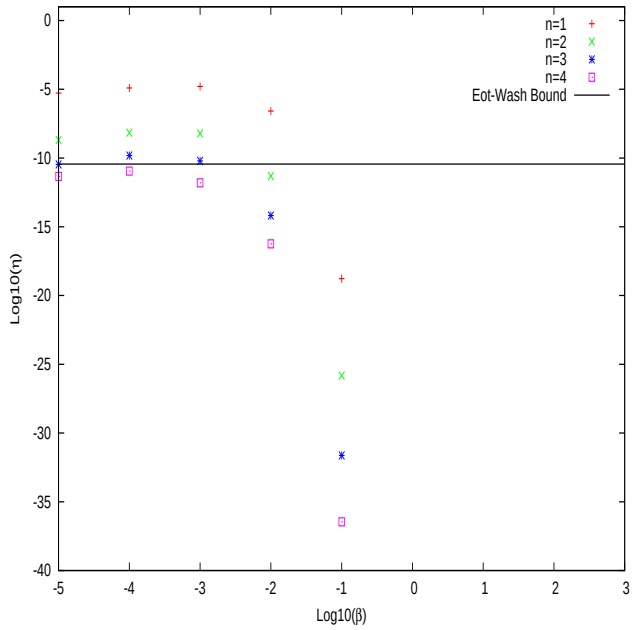

(a) η results for $\rho_{\rm out} = 10^{-7}$g cm^{-3}

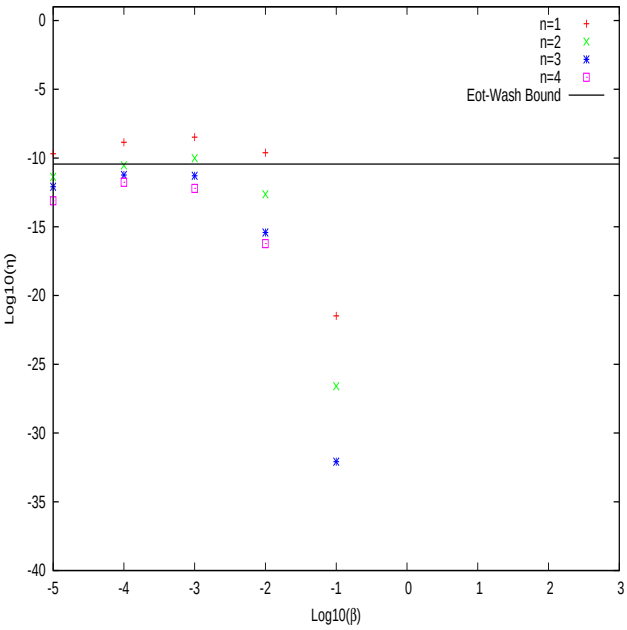

(b) η results for $\rho_{\rm out} = 10^{-3}$g cm^{-3}

Figure 6: The Eötvös parameter η (in $\log_{10}$ scale) as a function of the parameter β (in $\log_{10}$ scale) including the Yukawa suppression due to the metal encasing of the vacuum chamber for different positive values of n. The density of the environment $\rho_{\rm out}$ is assumed to be equal to: Panel (a) the vacuum's density inside the vacuum chamber $\rho_{\rm out} = 10^{-7}$g cm^{-3}; Panel (b) the Earth's atmosphere density $\rho_{\rm out} = 10^{-3}$g cm^{-3}

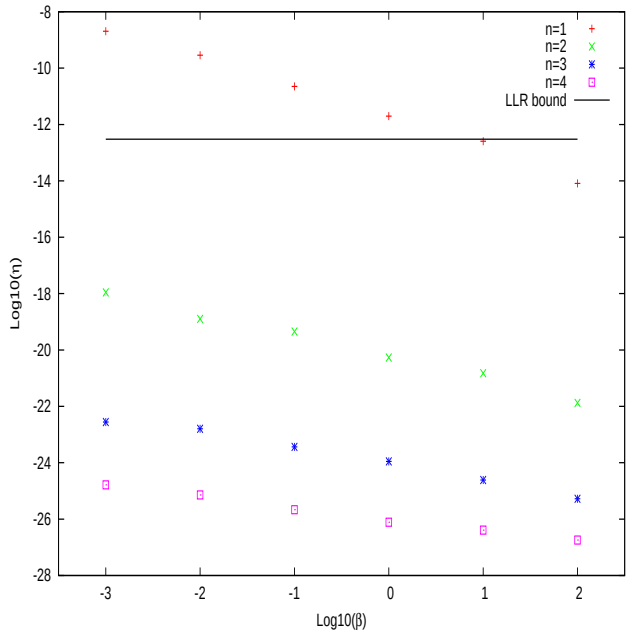

(a) η results for $M = 120$ cm^{-1}

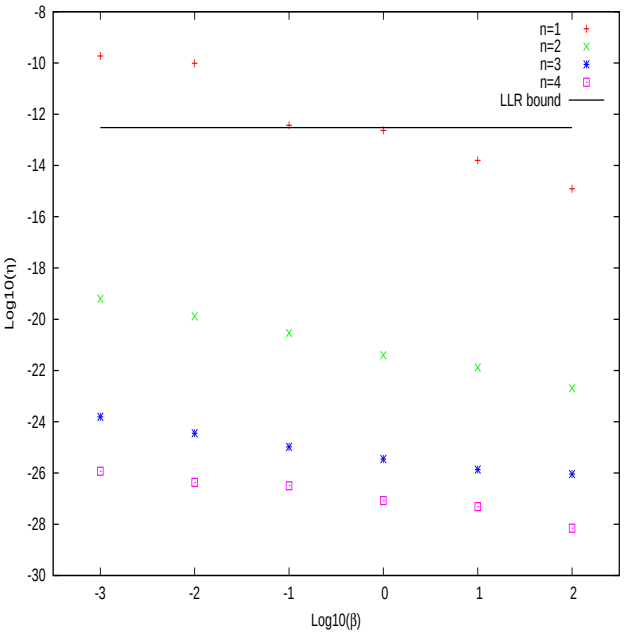

(b) η results for $M = 120$ cm^{-1}

Figure 7: The Eötvös parameter η (in $\log_{10}$ scale) for the Lunar Laser Ranging experiment as a function of the parameter β (in $\log_{10}$ scale) for different positive values of n. Panel (a) all bodies are surrounded by the interstellar medium; Panel (b) The Earth and the Sun are surrounded by two regions of constant density $\rho_{\rm out1} = \rho_{\rm atmosphere}$ and $\rho_{\rm out2} = \rho_{\rm interstellar}$ while the Moon is surrounded by the interstellar medium.

Table II: Differences in acceleration between the Earth and the Moon. Earth and Sun are surrounded by two regions of constant density $\rho_{\rm out1} = \rho_{\rm atmosphere}$ and $\rho_{\rm out2} = \rho_{\rm interstellar}$ while the Moon is surrounded by the interstellar medium

M	$\eta_{\rm n=1}$	$\eta_{\rm n=2}$	$\eta_{\rm n=3}$	$\eta_{\rm n=4}$
(1)	(2)	(3)	(4)	(5)
120.695	3.23×10^{-13}	1.35×10^{-21}	5.88×10^{-26}	1.39×10^{-27}

Notes.- Columns: (1) value of the parameter M in cm^{-1}, (2), (3), (4) and (5) differences in acceleration between the Earth and the Moon for $n = 1, 2, 3, 4$ respectively. The Eötvös parameter η is tabulated for a fixed value of $\beta = 1/\sqrt{6}$.

Table III: Differences in acceleration between the Earth and the Moon. All bodies are surrounded by the interstellar medium

M	$\eta_{\rm n=1}$	$\eta_{\rm n=2}$	$\eta_{\rm n=3}$	$\eta_{\rm n=4}$
(1)	(2)	(3)	(4)	(5)
120.695	1.17×10^{-11}	1.78×10^{-20}	2.82×10^{-24}	1.41×10^{-26}

Notes.- Columns: (1) value of the parameter M in cm^{-1}, (2), (3), (4) and (5) differences in acceleration between the Earth and the Moon for $n = 1, 2, 3, 4$ respectively. The Eötvös parameter η is tabulated for a fixed value of $\beta = 1/\sqrt{6}$.

V. SUMMARY AND CONCLUSIONS

In this paper, we have solved the chameleon field equation in the presence of two bodies (a larger body and a test body) and an environment. This has allowed us to evaluate the chameleon mediated force between these bodies and to determine the differential acceleration on two test bodies towards the larger one, resulting from the chameleon mediated interaction, which in turn can be compared with the outcome of the WEP experiments on Earth.

The approach that we have followed to compute the force takes into account that both bodies (the larger and smaller ones) contribute to determine the static field configuration everywhere. In order to simplify the calculations we have considered a scenario where the coupling between the chameleon field and the matter fields is universal. Furthermore, apart from the standard approximation made in characterizing the effective potential for the chameleon field as a quadratic one around its minimum, the only relevant approximation that has been made is to cutoff the series expansions of the development in spherical harmonics of the chameleon field. In the selection of the adequate cutoff in the series, we have followed the approach proposed in Refs. [24] and [25]. We have found that the force on the test body depends on the test body size and composition, making the model susceptible to experimental constrains arising from tests of the WEP, and thus, our conclusions differ drastically from previous studies which claim that the chameleon model predicts essentially no effective violation of the WEP whenever the thin shell regime ensues. The specific source of the difference between our calculations and the ones that predict no effective violation of WEP in chameleon models is that in those works [13, 15, 16], it is assumed that if the bodies involved produce the thin shell effect, the force mediated by the chameleon field would be automatically suppressed to such an extent as to make it irrelevant. By performing a careful and detailed calculation we have shown that this is not always the case. Regarding the situation where the coupling between the chameleon and the matter fields is universal, we must remind the reader that it is only when test objects are considered as true *point* particles which follow geodesics (as opposed to "test" extended bodies) that one might conclude that the model predicts no violation of bounds set by tests of the WEP. However such point test particles cannot be the ones that lead to thin shell effects. The analysis of the validity of a direct extension of that notion for a realistic extended body is highly non trivial and the calculations performed in this paper show that this issue is rather delicate and very relevant for the case of chameleon models.

Finally, we have quantitatively estimated the differential acceleration for test bodies made of Be and Al for one of the most precise experiments yielding relevant bounds considering two possibilities for the outside medium. On the other hand, we have included the effect of the vacuum's chamber metal shell in the prediction of violation of bounds

set by tests of the WEP , and found that expected violation of the WEP is suppressed beyond the experimental bounds for $\beta > 10^{-2}$. Unlike previous works [13, 15–17, 35] where it was assumed that the *thin shell* effect in high density environments prevents the prediction of violation of bounds set by tests of the WEP, we have shown that the absence of violation of the WEP in Eötvös-like experiments arises from the Yukawa-like suppression due to the vacuum's chamber metal shell. This point was noted earlier by Burrage et al. [40] studying atom interferometry in chameleon models. This authors showed that the effects of external sources are suppressed by the vacuum encasing, but a force can be produced using a source mass inside. This idea was applied by Hamilton et al. [34] who used a cesium matter-wave interferometer near a spherical mass in a ultra-high vacuum chamber to test chameleon models with individual atoms. However, it is important to stress that in this kind of experiments atoms are the test particles and therefore the whole point raised in this paper (and pointed out also by Ref. [17]) about the importance of considering a test body rather than a test particle is not applicable. In summary, experiments where both large and test bodies are not within a vacuum chamber are better candidates to be used in tests of violations of the WEP than Eötvös type experiments. Consequently, we have also considered the LLR where there is no encasing of the test bodies; for this experiment we find that the the prediction of effective violation of the WEP do not conflict with the existing experimental bounds, for $\beta > 10^{-1}$. As commented before, Upadhye has also analyzed the prediction of the chameleon model for tests of the gravitational inverse-square law where the matter distribution can be considered as one-dimensional and planar. From this analysis, the following combination of parameters are excluded by the WEP experimental tests: i) $-5.5 < n < 0$ and $\beta > 0.5$; ii) $n > 0$ and $0.01 < \beta < 10$ (for further details see Fig. 12 of Ref [35]). Therefore, the constraints on the chameleon model obtained in this paper are complementary to the ones found by Upadhye.

On the other hand, it is important to compare our conclusions with the results obtained by other experiments that also have put strong bounds on the free parameters of the chameleon model. Just to mention some of them: i) the search for solar chameleon with the CERN Axion Solar Telescope (CAST) using the Primakov effect [36], ii) "afterglow" experiments, a search for chameleon particles created via photon/chameleon oscillations within a magnetic field [37] and iii) resonance spectroscopy measurements of quantum states of ultra-cold neutrons [38] and iv) the above mentioned atom interferometer implemented by Hamilton et al.[34]. It should be mentioned, that all those experiments are also able to test an additional parameter, namely, the chameleon to photon coupling β_γ. The above mentioned experiments provide complementary bounds that those placed in this work, namely, they rule out the chameleon model for $\beta > 10^5$.

These results show that the chameleon model must be used with much more care than what is usually employed. In fact this work should alert colleagues who are under the impression that the chameleon effect, completely and effectively protects the model from having to confront these strict experimental bounds. Moreover given these results, various models that rely on the chameleon effect, should only be considered with the various specific values of n and β that are not, at this point ruled out by experiments. In this regard, it is important to emphasize that the viability of other modified theories which have been proposed to account for the accelerated expansion of the universe, often rely on the chameleon or *thin shell* effects in order to avoid the stringent bounds imposed by the *classical tests of general relativity*. However, many of such theories have not been yet confronted with the Eötvös type of bounds, as it is often taken for granted that the chameleon effect will suppress possible effective violations of the WEP, or because one assumes that such violations are not even present given the fact that metric alternative gravity theories have the WEP incorporated in them, like in general relativity. We think that, in view of the present results, the viability of those theories might be in serious jeopardy. Among such theories, one finds various types of $f(R)$ gravity theories as some of the most notorious examples. The point is that even if the chameleon (through the thin shell effect) is able to allow theories to pass the solar-system tests (as concluded by several authors [33]), the same mechanism can result in concomitant violations of the WEP far larger than the experimental bounds in the way we have discussed in this work. Moreover, violations of the WEP can be present as well in much more larger scales (like in galaxies) as was argued in [17]. In light of these conclusions, we consider that all such theories require a new and a deeper scrutiny regarding their empirical viability.

Acknowledgments

We would like to thank P. Brax, J. Khoury, A. Upadhye and B. Elder for very valuable private communications that helped us improve this manuscript. L.K. and S.L. are supported by PIP 11220120100504 CONICET and grant G119 UNLP. M.S. is partially supported by UNAM-PAPIIT grant IN107113 and CONACYT grants CB-166656 and CB-239639. D.S. is supported in part by the CONACYT grant No. 101712. and by UNAM-PAPIIT grant IN107412.

Appendix A: Clarifications

As a complement to our analysis of the problem, it is worth clarifying a couple of issues that often lead to misunderstandings in the discussion of these kind of theories. One of them, which often causes significant confusion in the context of theories involving chameleons or related type of *screening* effects, is the question of "passing to the test particle limit", while starting from the full *two body* problem. It is perhaps worthwhile to consider the corresponding question in the case of pure GR.

Let us assume we have the exact equation representing the spacetime metric for two extended bodies. If we do not want to complicate the problem by considering the external forces needed to keep these bodies at rest despite their mutual gravitational interaction, we might think of initial data on a spatial hypersurface Σ corresponding to a moment of time symmetry for the spacetime metric, together with a similar data for the matter part described in terms of their energy-momentum tensor associated with the two bodies. That is, we can consider initial data on Σ of the form $\{h_{ab}, K_{ab} = 0 = J_a\}$, where the quantities within the brackets correspond to the 3-metric on Σ, its extrinsic curvature and the momentum density current of matter, respectively. The gravitational part of this data is found by solving the Hamiltonian constraint with initial densities and pressures, whereas the momentum constraint is satisfied trivially by this choice of initial data. We can then obtain a full fledged self-consistent solution representing the spacetime together with the two extended objects in it, at least in a small neighborhood of the initial surface. With this at hand we might consider computing the instantaneous gravitational "force" on the bodies by solving the coupled gravitation and fluid equations, determining the center-of-mass world lines of the two bodies and computing the instantaneous initial acceleration of the center of mass of each body. The difficulties one would face in such program would include among others, those intrinsically associated with the general relativistic definition of the center of mass of an extended body.

With this setting in mind, let us consider taking the limit where the size of one of the objects shrinks to zero while keeping the density constant. By doing so we clearly reduce the contribution of the smaller body to the total gravitational field. In principle one expects to find that such contribution goes to zero in that limit, and thus such calculation might be viewed as recovering the standard GR conclusion that test particles should follows geodesics (curves with zero proper acceleration). As those geodesics are independent on the test-particle's composition, it is clear that the model predicts no violation of bounds set by tests of the WEP.

The task is however no so trivial when taking into account the "structure" of the smaller body [18, 20]. For instance, it turns out that even in the point-particle limit the persistence of an intrinsic spin leads to the appearance of a corrective force that will lead to a non-universality of free fall. Alternatively, one can adopt a posture that a particle with spin cannot be considered as a point particle[19].

Let us turn now to the second issue which concerns the type of theories under consideration here. The first observation is that in the general case where we have multiple β_i's we would be dealing with a multiplicity of physical metrics, one for each kind of matter field. Thus, presumably point particles of various kinds, will in principle, move on different types of world lines. Therefore it would make sense computing the force (or proper acceleration) on a point test particle of type 1 as it would be observed by devices made of matter of type 2. That is, we can in principle consider determining the spacetime metric associated with matter fields of type 2, and then determining the proper acceleration of a world line of a point particle of type 1, as described in that first metric. Moreover, we could determine the proper acceleration of the center of mass of an extended body made out of matter of type 1 and consider the limit as such test body shrinks to a point. Nonetheless in that instance we would not automatically recover a vanishing proper acceleration. However, when there is a single physical metric coupled minimally to the matter fields one, of course, expects that, in the point-particle limit, all test objects would follow the unique geodesics associated with that metric and, thus, that in that case there would not be any possibility of violation of the tests of the WEP. As a test of self-consistency, we have checked that this is obtained in the present analysis of the chameleon models (see Appendix C). On the other hand we have found that for some relevant experimental situations where the actual test objects cannot be considered as simple point particles, our analysis leads to predictions of observable effective violations of the WEP, and that these predictions are in conflict with experimental data.

In short the main points we must keep in mind to avoid confusion are the following: i) The case of universal β and ii) the test particle limit.

1. **Universal** β: This is the case where the various β_i associated with the various matter fields take the same universal value β. In this scenario all the various metrics $g^{(i)}_{\mu\nu}$ coalesce into a single metric, which we will denote

[19] This is a position that can be supported by noting that at the classical level there is indeed a lower bound to the size of a particle with a given mass and angular momentum (see Ref.[20]). Things of course become even more subtle at the quantum level.

by $g^{\rm J}_{\mu\nu}$. In that situation, it might seem that, as all matter fields couple to this metric in a single and universal manner, one should not expect any kind of effect that could be considered as a violation of the WEP. This would seem to contradict our findings (see Sec. III) that indicate that existing experiments on the WEP would have been seen the effects of the chameleon if it existed, even in the case of universal β (unless of course β were extremely small). The point, however, is that in the regime where the thin shell effect becomes relevant, the physical objects used in the experiments could not be considered to be simple test bodies, which move under the influence of an external spacetime metric, and have negligible effect on it. That is, the strong spatial variation of the scalar field inside such bodies that is associated with the thin shell effect, implies that the effects of the object on the spacetime metric $g^{\rm J}_{\mu\nu}$ can not be ignored. Thus the objects, must be considered as large extended objects, which are known (even in standard general relativity) not to follow geodesics [18, 20]. In such situation, where the effects of the objects with which one probes the spacetime have non-negligible effects on the metric one cannot argue that their motion would be independent of their structure and composition, and therefore in those cases there is no contradiction between the violation of the universality of free fall, and the fact that the coupling of matter to the spacetime metric is universal. Hence, one can either, discard the arguments based on the universal coupling of all matter fields to a single metric as protecting the model against test of the WEP, or one can argue that such protection arises from the chameleon effects, but one can not use both arguments simultaneously.

2. **The test particle limit**: the analysis of the conditions under which a certain body can be considered as a test particle are rather nontrivial [21], and involve examining the effects of the body on the spacetime metric. One type of analysis is based on the consideration of the "gravitational self-energy " of the body. However, this analysis requires extreme care, simply because such notion is not well defined in GR and similar theories. In the situation at hand, things become even more involved because, even if under certain circumstances one can come up with a reasonable definition of that notion, it is clear that such conception would be connected with each of the various spacetime metrics that appear in the theory ($g_{\mu\nu}$ and $g^{(i)}_{\mu\nu}$ or $g_{\mu\nu}$ and $g^{\rm J}_{\mu\nu}$ in the case of universal coupling β). We should also be careful with the conceptual differences between the *weak* and *strong* equivalence principle which become entangled in any theory (such as the one under consideration) possessing more than one metric.

Finally we note that for the case of universal β and in the test (point) particle limit, the model will not predict any violation of the WEP. Such situation clearly involves no chameleon effects and (at least for the test point particles) no spacetime variation of effective coupling constants, and thus has not been considered any further in this work, except for checking the self-consistency of our approach (cf. Appendix C)

Appendix B: The expanded solution

The results presented in Section IV have been calculated taking only the first ($N = 0$, $l = 0$) terms in the truncated series for the expression of the force. Here we show that taking two more terms (up to $N = 4$, $l = 4$), the results are basically the same. We only take two more terms because the larger the number of terms we take, the more unstable the numerical calculation becomes. On the other hand, the terms in the summations decrease several orders of magnitude when $l \neq 0$ and $w \neq 0$, so they do not really contribute to the result. Eqs. (18), (22), (26) and (27) yield

$$b_1\delta_{l0} = C_l^{\rm out1}a_l + \sum_{w=0}^{4} C_w^{\rm out2} z_{wl}, \tag{B1a}$$

$$b_2\delta_{l0} = C_l^{\rm out2}x_l + \sum_{w=0}^{4} C_w^{\rm out1} y_{wl}, \tag{B1b}$$

$$C_l^{\rm in1} i_l'(\mu_1 R_1) = C_l^{\rm out1} k_l'(\mu_{\rm out} R_1) + \sum_{w=0}^{4} C_w^{\rm out2} \alpha_{l0}^{w0} i_l'(\mu_{\rm out} R_1), \tag{B1c}$$

$$C_l^{\rm in2} i_l'(\mu_2 R_2) = C_l^{\rm out2} k_l'(\mu_{\rm out} R_2) + \sum_{w=0}^{4} C_w^{\rm out1} \alpha_{l0}^{*w0} i_l'(\mu_{\rm out} R_2); \tag{B1d}$$

Then, using these truncated series ($N = 4$) in the expressions for $F_{1{\rm z}\Phi}$ and $F_{2{\rm z}\Phi}$, we obtain the same results that we have shown in Section IV, but stress that the numerical calculation for the acceleration of the test body becomes very unstable for small values of β. Therefore, we only compute the force for β within the regime of the *thin shell*.

Appendix C: The test particle limit

In this appendix we show what happens in our proposal when the radius, R_2, of the test body tends to zero while the density ρ_2 (and μ_2) remain constant. First, we did this numerically within the approach presented in Section II A and confirmed that there are no violations of the WEP when the thin shell condition in the larger body ensues.

We implement two simplified models that provide more insight about this limit. In the first one, we take the chameleon field outside the test body to be that due to the larger body alone (which is easily found) and thus we require only to compute the field inside the test body. In the second model, we assume ab initio that the test body is literally a *test point particle*, and thus, that it does not produce any back-reaction on the larger body and the environment. Hence, we take the chameleon as generated solely by these two sources. That is, in this case the problem reduces to the usual one body problem (OBP) that has been studied in the past, and which corresponds to the static and spherically symmetric solution of the chameleon equation with one body surrounded by an environment.

So let us start analyzing the first of these two models that we call the simplified two body problem (STBP). Under the STBP we take the OBP solution in the outside region and inside the larger body (see Appendix D for a review on the OBP solution). However, inside the test body we consider the solution that matches continuously on its boundary with the exterior field. In order to do this we take the most general regular solution of the differential equation in that region, which is given by

$$\Phi_{\rm in2}(r',\phi',\theta') = \Phi(r',\phi',\theta') = \sum_{lm} C^{in2}_{lm} i_l(\mu_2 r') Y_{lm}(\theta',\phi') + \Phi_c^{\text{test body}} \qquad (r' \leq R_2) \ , \tag{C1}$$

where R_2 is the radius of the test body, and the primed spherical coordinates are taken with respect to a frame of reference centered at the origin of the test body. Like in the analysis of Section II A, inside the test body we consider only the MSBF's of the first type $i_l(.)$ which are regular at $r'=0$ as opposed to the MSBF's of second type $k_l(.)$, which are regular at infinity. We have introduced the notation $\Phi_c^{\text{test body}} = \Phi^{\rm in}_{\rm 2min}$, for the minimum of $V_{\rm eff}(\Phi)$ inside the test body, and similarly, $\mu_2 = m_{\rm eff}^{\text{test body}}$. In fact, the STBP that we analyze is *axially symmetric* (i.e. symmetric around the $z-axis$ that connects the centers of the two bodies as shown in Figure 1), thus, we need only the coefficients with $m=0$ (the others vanish identically).

As we indicated, here we take the chameleon outside the test body to be well approximated by the exterior field of the OBP (see Appendix D):

$$\Phi^{\rm out}(r) = C\frac{\exp\left[-\mu_{\rm out} r\right]}{r} + \Phi_\infty \ , \tag{C2}$$

where $\mu_{\rm out} = m_{\rm eff}^{\rm out}$ is the effective mass of the chameleon associated with the environment, $\vec{r}\,' = \vec{r} - D\hat{z}$, D is the distance between the centers of the two bodies (see Figure 1) and C is a constant that is found when matching the exterior with the interior solution of the OBP (see Appendix D). Let us remind that in the STBP we are ignoring the effect of the test body on the exterior solution, thus, for the STBP we only require the exterior solution of the larger body as if the test body were absent. The coefficients of the expansion in Eq. (C1) are found by matching this solution with the exterior solution Eq. (C2) at R_2. In order to do so we shall employ the following identity to rewrite $\Phi^{\rm out}(r)$ in terms of the coordinate system centered at the test body:

$$\frac{\exp\left[-\mu_{\rm out}|\vec{r}_2 - \vec{r}_1|\right]}{4\pi|\vec{r}_2 - \vec{r}_1|} = \mu_{\rm out}\sum_{l=0}^{\infty} i_l(\mu_{\rm out} r_2) k_l(\mu_{\rm out} r_1) \times \sum_{m=-l}^{l} Y_{lm}(\theta_2,\phi_2) Y^*_{lm}(\theta_1,\phi_1),$$

as long as $r_2 < r_1$ and being $k_l(.)$ the MSBF of second type mentioned previously. In the current case $\vec{r}_1 = -D\hat{z}$, $\theta_1 = 0$, and $\vec{r}_2 = \vec{r}\,'$. As mentioned before only the terms with $m=0$ contribute to the solution. The matching condition $\Phi_{\rm in2}(R_2) = \Phi_{\rm out}(R_2)$, leads to

$$C^{\rm in2}_{l0} = \left[\frac{(\Phi_\infty - \Phi_c^{\rm tbody})\delta_{l0}}{2l+1} + C\mu_{\rm out} i_l(\mu_{\rm out} R_2) k_l(\mu_{\rm out} D)\right] \times \frac{\sqrt{4\pi(2l+1)}}{i_l(\mu_2 R_2)}. \tag{C3}$$

Remarkably, even at this level of approximation, and despite considering the case of a universal coupling β, Eq. (C3), shows that the field inside the test body depends on the test body properties, like its size R_2 and composition [both μ_2 and $\Phi_c^{\rm tbody}$ depend on $\rho_{\rm tbody}$ according to Eqs. (11) and (12)]. This result is at odds with the findings of other authors [13, 16]. As soon as ones considers test bodies as extended bodies, they can be an important source of the chameleon, and as such, their composition appears naturally in the detailed behavior of the scalar field. It is important to emphasize that in this STBP we cannot longer impose the continuity of the first derivative of the chameleon at R_2.

This discontinuity can produce serious consequences in the resulting force when the test body is of finite size. This is why we do not use this simplified model for that purpose. Nonetheless, in the limit $R_2 \to 0$ this drawback disappears.

Now, we want precisely to consider this limit. First, the coefficient of the chameleon in spherical harmonics with $l = 0$ associated with the solution due to the larger body behaves as follows

$$C_{00}^{\rm in1} \sim \frac{\sqrt{4\pi}\mu_1(1+\mu_{\rm out}R_1)(\Phi_\infty - \Phi_{\rm 1min}^{\rm in})\,{\rm csch}(\mu_1 R_1)}{\mu_{\rm out} + \mu_1 \coth(\mu_1 R_1)}, \tag{C4a}$$

$$C_{00}^{\rm out1} \sim \frac{\sqrt{4\pi}\exp[\mu_{\rm out}R_1]\mu_{\rm out}(\Phi_\infty - \Phi_{\rm 1min}^{\rm in})\{\mu_1 R_1\cosh(\mu_1 R_1) - \sinh(\mu_1 R_1)\}}{\mu_1\cosh(\mu_1 R_1) + \mu_{\rm out}\sinh(\mu_1 R_1)}, \tag{C4b}$$

$$C_{00}^{\rm out2} \sim 0. \tag{C4c}$$

By construction, the chameleon field inside the larger body and outside both bodies does not depend on anything coming from the test body. On the other hand, the coefficient $C_{00}^{\rm in2}$ of Eq. (C3) in the limit $R_2 \to 0$ becomes,

$$C_{00}^{\rm in2} \sim \sqrt{4\pi}\Big\{(\Phi_\infty - \Phi_{\rm 2min}^{\rm in}) + \frac{\exp[\mu_{\rm out}(R_1 - D)](\Phi_\infty - \Phi_{\rm 1min}^{\rm in})[\sinh(\mu_1 R_1) - \mu_1 R_1\cosh(\mu_1 R_1)]}{D[\mu_1\cosh(\mu_1 R_1) + \mu_{\rm out}\sinh(\mu_1 R_1)]}\Big\}. \tag{C5}$$

So, the field $\Phi_{\rm in2}(\vec{r'})$ when $R_2 \to 0$ becomes

$$\Phi_{\rm in2} \sim \Phi_\infty + \frac{\exp[\mu_{\rm out}(R_1 - D)](\Phi_\infty - \Phi_{\rm 1min}^{\rm in})[\sinh(\mu_1 R_1) - \mu_1 R_1\cosh(\mu_1 R_1)]}{D[\mu_1\cosh(\mu_1 R_1) + \mu_{\rm out}\sinh(\mu_1 R_1)]}; \tag{C6}$$

Thus, it follows from the above equations that in this limit the chameleon field does not depend on the test particle composition, and thus, there is no effective violation of the WEP.

Let us now consider a different simplification, where the test body is taken as a test point particle from the very beginning. This is what one usually finds in most of the literature. Since one takes the test body as test particle and the larger body and the environment as spherical sources of different uniform densities, one takes the following distribution for the matter part, $T^m \approx -\rho = -\mathcal{M}_2\delta(z-D)\delta(x)\delta(y) - \rho_{\rm in}^1\Theta(r-R) - \rho_{\rm out}\tilde{\Theta}(r,R)$, where $\mathcal{M}_2$ is the mass of the test body, and the step function $\tilde{\Theta}(r,R)$ is defined to be unity for $R < r < \infty$ and zero otherwise. The distribution $\rho_{\rm out}\tilde{\Theta}(r,R)$ allows one to describe the environment of density $\rho_{\rm out}$.

Therefore from Eq. (34) we obtain

$$U_\Phi \approx \Phi_{\rm out}(\vec{r})\frac{C_n\beta\mathcal{M}_2}{M_{pl}} + {\rm const.} \tag{C7}$$

where $\vec{r}$ corresponds to the location of the point-test particle, and the constant contains information about the bulk properties of the larger body, the environment and the point-test particle, but it is independent of the location of the latter. Thus the only contribution for the force arises only from the term in the integral of Eq. (34) that is proportional to $\hat{\Phi}T^m$, which contains the information of the chameleon and the location of the test body. Here $C_n = (n+3)/2$.

In this way, the chameleon force on the point-test particle reads

$$\vec{F} = -\vec{\nabla}U_\Phi = -\frac{C_n\beta\mathcal{M}_2}{M_{pl}}\vec{\nabla}\Phi_{\rm out}\ , \tag{C8}$$

again, this is to be evaluated at the location of the point-test particle. Henceforth, apart from the factor C_n, we recover the same expression considered in [13] for the chameleon force acting on a point test-particle.

Now, in this limit the solution for the chameleon is given by Eq. (C2), which is the exterior solution of the one body problem in spherical symmetry. In order to give an insight of the Eötvös parameter and the way it can be constrained when a thin shell exists, it is better to take the constant C of Eq. (C2) as written in the form Eq. (D3). As explained in Appendix D below, when there is a thin shell the exterior solution reads [cf. Eq. (D3) with $f(x) \approx 1$]

$$\Phi^{\rm out}(r) \approx \Phi_\infty - \frac{3\beta\mathcal{M}}{4\pi M_{pl}}\frac{\Delta R}{R}\frac{\exp\left[-m_{\rm eff}^{\rm out}(r-R)\right]}{r}\ . \tag{C9}$$

where $\mathcal{M}$ is the mass of the large body. For simplicity let us assume $r \sim R$ and $m_{\rm eff}^{\rm out}(r-R) \ll 1$. Thus

$$\Phi^{\rm out}(r) \approx \Phi_\infty - \frac{3\beta}{4\pi M_{pl}}\frac{\Delta R}{R}\frac{\mathcal{M}}{r}\ . \tag{C10}$$

Using this expression in (C8) the chameleon force on the point-test particle at distance $r = D$ turns out to be

$$\vec{F}_\phi = -\hat{r}\frac{3C_n\beta^2}{4\pi M_{pl}^2}\frac{\Delta R}{R}\frac{\mathcal{M}\mathcal{M}_2}{D^2} \ , \tag{C11}$$

where $\hat{r}$ is the unit radial vector. Notice that the chameleon force is proportional to the gravitational force acting on the particle due to the larger body

$$\vec{F}_g = -\hat{r}\frac{G\mathcal{M}_G\mathcal{M}_{G,2}}{D^2} \ , \tag{C12}$$

where $\mathcal{M}_G$ and $\mathcal{M}_{G,2}$ are the *gravitational* masses of the larger body and the point-test particle, respectively, as opposed to their *chameleon*-like masses (or "chameleon charges") $\mathcal{M}$ and $\mathcal{M}_2$. That is, the masses that couple to the chameleon force.

In this way, the magnitude of the acceleration of the point-test particle due to the larger body is

$$a_2 = \frac{|\vec{F}_\phi + \vec{F}_g|}{\mathcal{M}_{I,2}} = \frac{G\mathcal{M}_G}{D^2}\left(\frac{\mathcal{M}_{G,2}}{\mathcal{M}_{I,2}} + \frac{6C_n\beta^2\mathcal{M}_2\mathcal{M}}{\mathcal{M}_{I,2}\mathcal{M}_G}\frac{\Delta R}{R}\right) \ , \tag{C13}$$

where $\mathcal{M}_{I,2}$ is the *inertial* mass of the point-test particle and we used $G = 1/(8\pi M_{pl}^2)$.

If the coupling to the chameleon force is not universal then this acceleration reads

$$a_2 = \frac{G\mathcal{M}_G}{D^2}\left(\frac{\mathcal{M}_{G,2}}{\mathcal{M}_{I,2}} + \frac{6C_n\beta_1\beta_2\mathcal{M}_2\mathcal{M}}{\mathcal{M}_{I,2}\mathcal{M}_G}\frac{\Delta R}{R}\right) \ . \tag{C14}$$

A similar expression is obtained for the acceleration of a second point-test particle except that the masses $\mathcal{M}_2, \mathcal{M}_{G,2}$ and $\mathcal{M}_2^I$ of the first point-test particle are replaced by the masses $\mathcal{M}_3, \mathcal{M}_{G,3}$ and $\mathcal{M}_3^I$ of the second point-test particle, and similarly β_2 is replaced by β_3.

Therefore the relative acceleration of two "free-falling" point-test particles under the influence of both gravity and the chameleon due to the larger body is

$$|a_2 - a_3| = \frac{G\mathcal{M}_G}{D^2}\left|\frac{\mathcal{M}_{G,2}}{\mathcal{M}_{I,2}} - \frac{\mathcal{M}_{G,3}}{\mathcal{M}_{I,3}} + \left(\frac{\beta_2\mathcal{M}_2}{\mathcal{M}_{I,2}} - \frac{\beta_3\mathcal{M}_3}{\mathcal{M}_{I,3}}\right)\frac{6C_n\beta_1\mathcal{M}}{\mathcal{M}_G}\frac{\Delta R}{R}\right| \ . \tag{C15}$$

The Eötvös parameter is thus given by

$$\eta = \frac{2|a_2 - a_3|}{a_2 + a_3} = 2\frac{\left|\frac{\mathcal{M}_{G,2}}{\mathcal{M}_{I,2}} - \frac{\mathcal{M}_{G,3}}{\mathcal{M}_{I,3}} + \left(\frac{\beta_2\mathcal{M}_2}{\mathcal{M}_{I,2}} - \frac{\beta_3\mathcal{M}_3}{\mathcal{M}_{I,3}}\right)\frac{6C_n\beta_1\mathcal{M}}{\mathcal{M}_G}\frac{\Delta R}{R}\right|}{\frac{\mathcal{M}_{G,2}}{\mathcal{M}_{I,2}} + \frac{\mathcal{M}_{G,3}}{\mathcal{M}_{I,3}} + \left(\frac{\beta_2\mathcal{M}_2}{\mathcal{M}_{I,2}} + \frac{\beta_3\mathcal{M}_3}{\mathcal{M}_{I,3}}\right)\frac{6C_n\beta_1\mathcal{M}}{\mathcal{M}_G}\frac{\Delta R}{R}} \ . \tag{C16}$$

Taking $\beta_i = 0$ $(i = 1 - 3)$ we recover the usual expression of this parameter only due to gravity. On the other hand, for $\beta_i \neq 0$ but assuming that the inertial and gravitational masses are the same, we obtain the Eötvös parameter due to the chameleon solely:

$$\eta = \frac{2|a_2 - a_3|}{a_2 + a_3} = \frac{\Delta R}{R}\frac{\frac{6C_n\beta_1\mathcal{M}}{\mathcal{M}_G}\left|\frac{\beta_2\mathcal{M}_2}{\mathcal{M}_{I,2}} - \frac{\beta_3\mathcal{M}_3}{\mathcal{M}_{I,3}}\right|}{1 + \left(\frac{\beta_2\mathcal{M}_2}{\mathcal{M}_{I,2}} + \frac{\beta_3\mathcal{M}_3}{\mathcal{M}_{I,3}}\right)\frac{3C_n\beta_1\mathcal{M}}{\mathcal{M}_G}\frac{\Delta R}{R}} \ . \tag{C17}$$

This expression is used to stress the importance of the thin shell condition $\Delta R \ll R$. If the equality between the chameleon-like mass and the inertial mass holds exactly as well, then the relative acceleration between the two point-test particles is only due to the difference $|\beta_2 - \beta_3|$ may not strictly vanish. Thus, if such a difference is of order unity, then the observations $\eta \sim 10^{-13}$ (or $\eta \sim 10^{-11}$ if one takes into account only the effects produced by the local inhomogeneities of the matter near the torsion balance) can be satisfied provided $\Delta R/R$ is small enough. This is the chameleon mechanism at work for the point-particle limit. Moreover, if the couplings β_i are universal, then $\eta \equiv 0$ regardless of whether the larger body is associated with a "thin shell" or not. As we stressed before, in the universal-coupling scenario we checked numerically that $\eta \to 0$ in our full model of Section II A as we reduced the size of the (extended) test body.

Summarizing, the standard assumption is that the *screening* effects produced by the chameleon behavior, effectively suppress the dependency of η on the the couplings β_i in models where this parameter is not universal. Nonetheless, as we have shown here such supposition seems to work only for the true point-particle limit of test bodies, but not at the more precise level of the current analysis which is the relevant one for consideration of actual experimental test, where the test bodies are not just point particles, but small bodies of finite size.

Appendix D: The one body problem solution for the chameleon

When solving Eq. (6) for the one body problem and its environment under similar assumptions of Section II A but in spherical symmetry, we find the following interior solution:

$$\Phi^{\rm in}(r) = \frac{(\Phi_0 - \Phi_c)\sinh(m_{\rm eff}^{\rm in} r)}{m_{\rm eff}^{\rm in} r} + \Phi_c \qquad (r \leq R) \ , \tag{D1}$$

where $\Phi_c := \Phi_{\rm min}^{\rm in}$ and the value of the scalar field at the origin is given by

$$\Phi_0 = \Phi_c + \frac{(\Phi_\infty - \Phi_c)\,[1 + m_{\rm eff}^{\rm out} R]}{\frac{m_{\rm eff}^{\rm out} R}{x}\sinh(x) + \cosh(x)},$$

with $x := m_{\rm eff}^{\rm in} R$. The exterior solution is

$$\Phi^{\rm out}(r) = C\frac{\exp\left[-m_{\rm eff}^{\rm out} r\right]}{r} + \Phi_\infty \qquad (r \geq R) \ , \tag{D2}$$

where

$$C = -\frac{3\beta\mathcal{M}}{4\pi M_{pl}}\frac{\Delta R}{R}\exp\left[m_{\rm eff}^{\rm out} R\right] f(x) \ , \tag{D3}$$

and

$$\frac{\Delta R}{R} \ = \ -\frac{4\pi M_{pl} R(\Phi_c - \Phi_\infty)}{3\beta\mathcal{M}} = -\frac{(\Phi_c - \Phi_\infty)}{6\beta M_{pl}\Phi_N} \ , \tag{D4}$$

$$f(x) \ := \ \frac{\left[\cosh(x) - \frac{\sinh(x)}{x}\right]}{\frac{m_{\rm eff}^{\rm out} R}{x}\sinh(x) + \cosh(x)} \ . \tag{D5}$$

$\frac{\Delta R}{R}$ is the so called *thin-shell parameter* introduced in [13], $\mathcal{M}$ and $\Phi_N = \frac{\mathcal{M}}{8\pi M_{pl}^2 R}$ are the mass and the Newtonian potential of the body, respectively.

These solutions are found by demanding the following requirements: i) regularity condition at $r = 0$, i.e., $\Phi^{\rm in}(0) = \Phi_0$, ii) continuity and differentiability at $r = R$, iii) the asymptotic condition $\Phi^{\rm out}(r \to \infty) = \Phi_{\rm min}^{\rm out} = \Phi_\infty$.

The so called *thin-shell* effect appears when $1 \ll m_{\rm eff}^{\rm in} R$. So, under the thin-shell regime the approximate expressions for the field inside and outside the body are:

$$\Phi^{\rm in}(r) \ \approx \ \frac{2(\Phi_\infty - \Phi_c)\exp\left[-R m_{\rm eff}^{\rm in}\right]\sinh(m_{\rm eff}^{\rm in} r)}{m_{\rm eff}^{\rm in} r} + \Phi_c \qquad (r \leq R) \ , \tag{D6}$$

$$\Phi^{\rm out}(r) \ \approx \ R(\Phi_c - \Phi_\infty)\frac{\exp\left[-m_{\rm eff}^{\rm out}(r - R)\right]}{r} + \Phi_\infty \qquad (r \geq R) \ . \tag{D7}$$

Notice that due to the exponential factor, the r dependence of $\Phi^{\rm in}(r)$ is strongly suppressed in regions well inside the body (i.e. $r \ll R$; where $\Phi^{\rm in}(r) \approx \Phi_c$), and it is only within a *thin shell* of size ΔR, which is near the surface of the body, that the field grows exponentially to match the exterior solution $\Phi^{\rm out}(r)$. In addition, when $1 \ll x$ one verifies that $f(x) \approx 1$ when the density contrast between the body and the environment is high.

This is the essence of the "chameleon effect": the *screening* effect that makes the chameleon to behave like the electric potential within a conductor.

Appendix E: Non linear corrections to the chameleon interaction and the perturbative analysis

1. Non linear perturbation to the chameleon in one body problem

In order to estimate the corrections introduced by the low order approximation used in the expansion of $V_{\rm eff}$ (Eq.(9)) we consider the effects of cubic term in the expansion as a perturbation for the one body problem. Consequently, the

expansion of the effective potential about the corresponding minimum in each region up to the cubic term gives:

$$V_{\rm eff}^{\rm in,out}(\Phi) \simeq V_{\rm eff}^{\rm in,out}(\Phi_{\rm min}^{\rm in,out}) \tag{E1}$$
$$+ \frac{1}{2}\partial_{\Phi\Phi}V_{\rm eff}^{\rm in,out}(\Phi_{\rm min}^{\rm in,out})[\Phi-\Phi_{\rm min}^{\rm in,out}]^2 \tag{E2}$$
$$+ \frac{\epsilon}{6}\partial_{\Phi\Phi\Phi}V_{\rm eff}^{\rm in,out}(\Phi_{\rm min}^{\rm in,out})[\Phi-\Phi_{\rm min}^{\rm in,out}]^3, \tag{E3}$$

being ϵ a dimensionless parameter that indicates only the order in which we are working. Next we introduce

$$\sigma_{\rm eff}^{\rm 3in,out}(\Phi_{\rm min}^{\rm in,out},\beta,T_{\rm in,out}^m) \equiv \partial_{\Phi\Phi\Phi}V_{\rm eff}^{\rm in,out}(\Phi_{\rm min}^{\rm in,out}). \tag{E4}$$

Replacing this new expansion of the effective potential in the equation of motion for the chameleon, we get;

$$\nabla^2\Phi = m_{\rm eff}^{\rm 2in,out}[\Phi-\Phi_{\rm min}^{\rm in,out}] + \frac{\epsilon}{2}\sigma_{\rm eff}^{\rm 3in,out}[\Phi-\Phi_{\rm min}^{\rm in,out}]^2. \tag{E5}$$

We now write $\Phi=\Phi_0+\epsilon\Phi_1$, so that at the zero-order in ϵ, the above equation becomes the situation that we have already studied earlier,

$$\nabla^2\Phi_0 = m_{\rm eff}^{\rm 2in,out}[\Phi_0-\Phi_{\rm min}^{\rm in,out}], \tag{E6}$$

for details see Appendix D. At next order in ϵ, the equation of motion is given by,

$$\nabla^2\Phi_1 = m_{\rm eff}^{\rm 2in,out}\Phi_1 + \frac{1}{2}\sigma_{\rm eff}^{\rm 3in,out}[\Phi_0-\Phi_{\rm min}^{\rm in,out}]^2; \tag{E7}$$

which is an inhomogeneous equation with boundary conditions. This kind of equations are solved using Green's theorem,

$$\nabla^2X(\mathbf{r}) - \kappa^2X(\mathbf{r}) = f(\mathbf{r}), \tag{E8a}$$
$$X(\mathbf{r}) = \int_S [G_w(\mathbf{r},\mathbf{r}^*)\frac{\partial X(\mathbf{r}^*)}{\partial\mathbf{n}^*} - X(\mathbf{r}^*)\frac{\partial G_w(\mathbf{r},\mathbf{r}^*)}{\partial\mathbf{n}^*}]dS^* - \int_V f(\mathbf{r}^*)G_w(\mathbf{r},\mathbf{r}^*)dV^*. \tag{E8b}$$

When corresponding Green function $G_w(\mathbf{r},\mathbf{r}^*)$ satisfies the same boundary conditions as the field on parts of the boundary; the two terms in the kernel of the surface integral are identical, eliminating the integral on that part of the boundary.

In our particular case where two different mediums (*in, out*) are involved, the Green functions that we have to use are the ones of third kind $G_{i,j}(\mathbf{r},\mathbf{r}^*)$; where i indicates the place for the field point and j for the source point (for details see [27–29]). So we have the following Green functions,

$$G_{\rm in,in}(\vec{r},\vec{r^*}), \qquad G_{\rm out,in}(\vec{r},\vec{r^*}),$$

$$G_{\rm out,out}(\vec{r},\vec{r^*}), \qquad G_{\rm in,out}(\vec{r},\vec{r^*}),$$

that should satisfy ($i\neq j$);

$$\nabla^2G_{i,i}(\vec{r},\vec{r^*}) - m_{\rm eff,i}^2G_{i,i}(\vec{r},\vec{r^*}) = -\delta(\vec{r}-\vec{r^*}), \tag{E9a}$$
$$\nabla^2G_{i,j}(\vec{r},\vec{r^*}) - m_{\rm eff,i}^2G_{i,j}(\vec{r},\vec{r^*}) = 0, \tag{E9b}$$
$$G_{i,i}(\vec{r},\vec{r^*})|_{r=R} = G_{j,i}(\vec{r},\vec{r^*})|_{r=R}, \tag{E9c}$$
$$\partial_rG_{i,i}(\vec{r},\vec{r^*})|_{r=R} = \partial_rG_{j,i}(\vec{r},\vec{r^*})|_{r=R}. \tag{E9d}$$
$$\tag{E9e}$$

$G_{\rm in,in}(\vec{r},\vec{r^*})$ and $G_{\rm in,out}(\vec{r},\vec{r^*})$ are finite in the origin, while $G_{\rm out,out}(\vec{r},\vec{r^*})$ and $G_{\rm out,in}(\vec{r},\vec{r^*})$ become null at infinite.

Fulfilling the above conditions and considering spherical symmetry we can find the Green functions that we

need,

$$G_{\rm in,in}(\vec{r},\vec{r^*}) = \frac{\exp[-m^{\rm in}_{\rm eff}|\vec{r}-\vec{r^*}|]}{4\pi|\vec{r}-\vec{r^*}|} + i_0(m^{\rm in}_{\rm eff}r)i_0(m^{\rm in}_{\rm eff}r^*)\frac{m^{\rm in}_{\rm eff}(m^{\rm in}_{\rm eff}-m^{\rm out}_{\rm eff})}{2\pi[(m^{\rm in}_{\rm eff}-m^{\rm out}_{\rm eff})+(m^{\rm in}_{\rm eff}+m^{\rm out}_{\rm eff})\exp[2m^{\rm in}_{\rm eff}R]]}, \tag{E10a}$$

$$G_{\rm out,out}(\vec{r},\vec{r^*}) = \frac{\exp[-m^{\rm out}_{\rm eff}|\vec{r}-\vec{r^*}|]}{4\pi|\vec{r}-\vec{r^*}|} + k_0(m^{\rm out}_{\rm eff}r)k_0(m^{\rm out}_{\rm eff}r^*)\frac{\exp[m^{\rm out}_{\rm eff}R]m^{\rm out}_{\rm eff}Z}{4\pi[m^{\rm in}_{\rm eff}\cosh(\mathrm{m^{in}_{eff}R})+\mathrm{m^{out}_{eff}}\sinh(\mathrm{m^{in}_{eff}R})]}, \tag{E10b}$$

$$G_{\rm out,in}(\vec{r},\vec{r^*}) = k_0(m^{\rm out}_{\rm eff}r)i_0(m^{\rm in}_{\rm eff}r^*)\frac{m^{\rm in}_{\rm eff}m^{\rm out}_{\rm eff}\exp[R(m^{\rm in}_{\rm eff}+m^{\rm out}_{\rm eff})]}{2\pi[(m^{\rm in}_{\rm eff}-m^{\rm out}_{\rm eff})+(m^{\rm in}_{\rm eff}+m^{\rm out}_{\rm eff})\exp[2m^{\rm in}_{\rm eff}R]]}, \tag{E10c}$$

$$G_{\rm in,out}(\vec{r},\vec{r^*}) = i_0(m^{\rm in}_{\rm eff}r)k_0(m^{\rm out}_{\rm eff}r^*)\frac{\exp[m^{\rm out}_{\rm eff}R]m^{\rm in}_{\rm eff}m^{\rm out}_{\rm eff}\mathrm{csch}(\mathrm{m^{in}_{eff}R})}{4\pi[m^{\rm out}_{\rm eff}+m^{\rm in}_{\rm eff}\mathrm{cotch}(\mathrm{m^{in}_{eff}R})]}; \tag{E10d}$$

with

$$Z = m^{\rm out}_{\rm eff}\cosh(m^{\rm out}_{\rm eff}R)\sinh(m^{\rm in}_{\rm eff}R) - m^{\rm in}_{\rm eff}\cosh(m^{\rm in}_{\rm eff}R)\sinh(m^{\rm out}_{\rm eff}R).$$

Therefore,

$$\Phi^{\rm in}_1(r) = -\int_{V_{\rm in}} G_{\rm in,in}(\vec{r},\vec{r^*})\sigma^{3\rm in}_{\rm eff}[\Phi^{\rm in}_0(r^*)-\Phi^{\rm in}_{\rm min}]^2 dV^*_{\rm in} - \int_{V_{\rm out}} G_{\rm in,out}(\vec{r},\vec{r^*})\sigma^{3\rm out}_{\rm eff}[\Phi^{\rm out}_0(r^*)-\Phi^{\rm out}_{\rm min}]^2 dV^*_{\rm out}, \tag{E11a}$$

$$\Phi^{\rm out}_1(r) = -\int_{V_{\rm in}} G_{\rm out,in}(\vec{r},\vec{r^*})\sigma^{3\rm in}_{\rm eff}[\Phi^{\rm in}_0(r^*)-\Phi^{\rm in}_{\rm min}]^2 dV^*_{\rm in} - \int_{V_{\rm out}} G_{\rm out,out}(\vec{r},\vec{r^*})\sigma^{3\rm out}_{\rm eff}[\Phi^{\rm out}_0(r^*)-\Phi^{\rm out}_{\rm min}]^2 dV^*_{\rm out}. \tag{E11b}$$

Now we can estimate the chameleon force in one body problem and compare with the one obtained with the linear solution. For this case, $\vec{F_\Phi} = -\frac{\beta M_c}{M_{pl}}\vec{\nabla}\Phi$. We consider F_T the force due to $\Phi_0(r)+\epsilon\Phi_1(r)$ and F_L the force due to $\Phi_0(r)$. In Figures 8 and 9 we represent the ratio of the difference between the total force and linear force, and linear force $\left|\frac{F_T(r)-F_L(r)}{F_L(r)}\right|$ as a function of β for different positive values of n. It can be seen that the above ratio increases with n, in such a way that, for $n>4$ the perturbation has the same order as the original (linear) term. Meanwhile, the increase in the ratio with β is noticeable when β is very small ; but when $\beta \geq 1$, the ratio becomes almost constant. It seems that when the density of the outside medium is higher, the ratio is lower; and so it is when we evaluate the forces at a finite distance outside from the body, rather than on its surface.

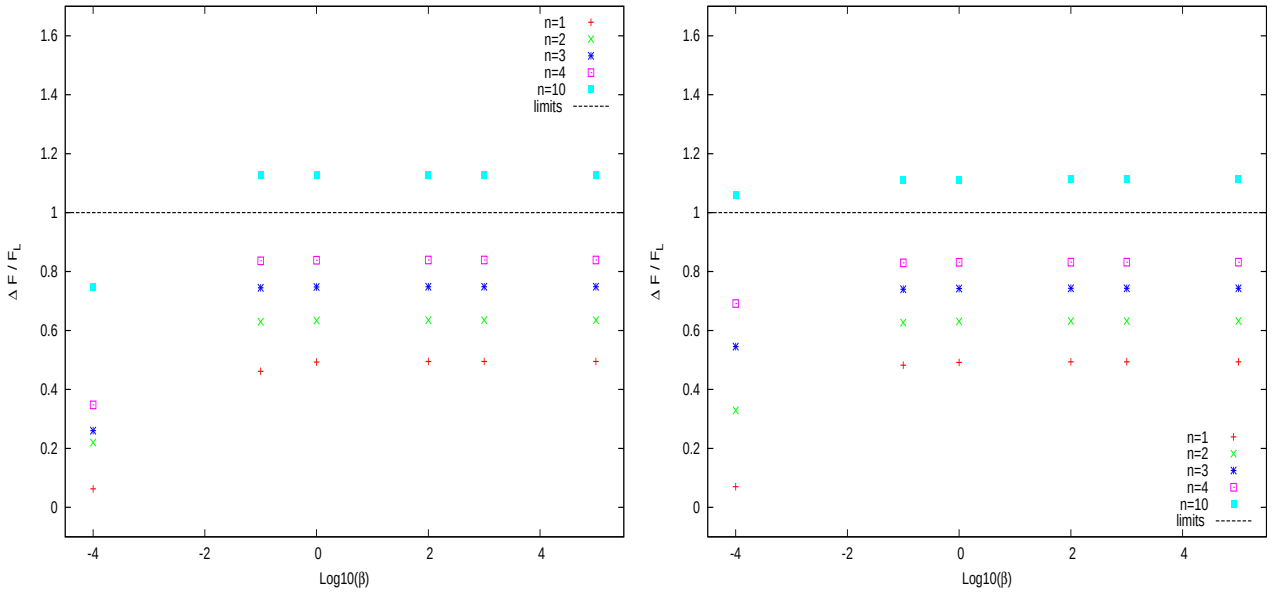

(a) $\frac{\Delta F}{F_L}$ results for $r = 1650$ cm

(b) $\frac{\Delta F}{F_L}$ results for $r = 1550$ cm

Figure 8: The ratio of the difference between the total force and linear force, and linear force for the Eöt-Wash experiment (Hill immersed in the Earth's atmosphere) as a function of the parameter β (in $\log_{10}$ scale) for different positive values of n. Panel (a) the forces are calculated at $r = 1650$ cm; Panel (b) the forces are calculated at the surface of the hill, $r = 1550$ cm.

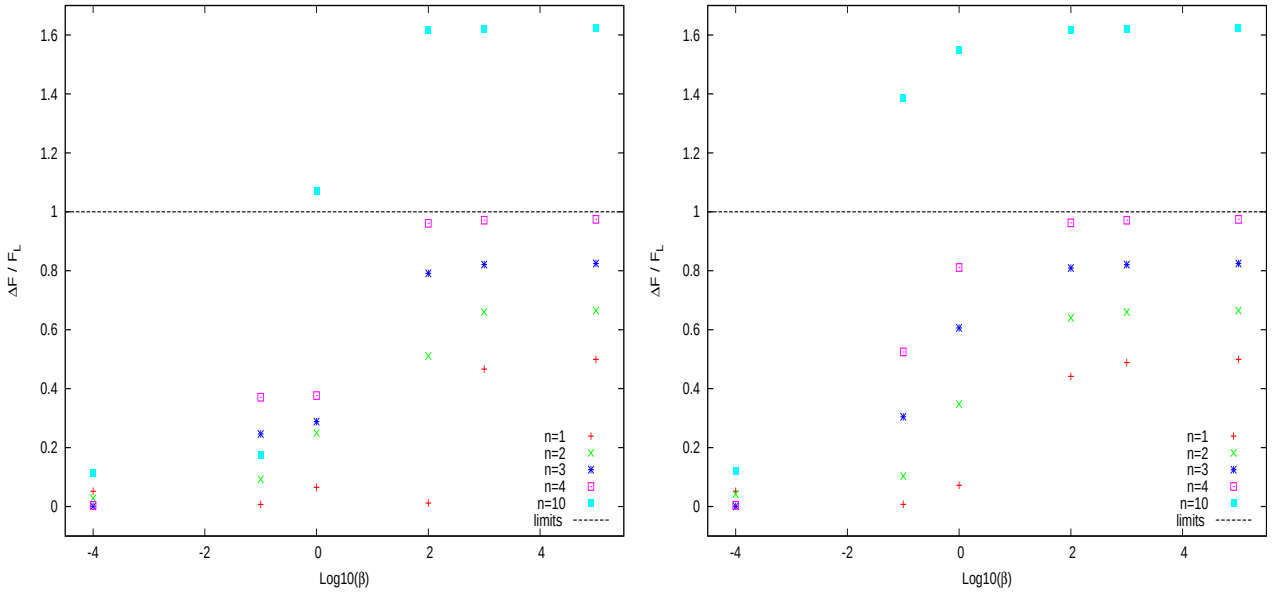

(a) $\frac{\Delta F}{F_L}$ results for $r = 1650$ cm (b) $\frac{\Delta F}{F_L}$ results for $r = 1550$ cm

Figure 9: The ratio of the difference between the total force and linear force, and linear force for the Eöt-Wash experiment (Hill immersed in the chamber's vacuum) as a function of the parameter β (in $\log_{10}$ scale) for different positive values of n. Panel (a) the forces are calculated at $r = 1650$ cm; Panel (b) the forces are calculated at the surface of the hill, $r = 1550$ cm.

[1] J. D. Bekenstein, Phys. Rev. D **25**, 1527 (1982)
[2] J. D. Barrow, J. Magueijo, and H. B. Sandvik, Phys. Rev. D **66**, 043515 (2002)
[3] K. A. Olive, and M. Pospelov, Phys. Rev. D **65**, 085044 (2002)
[4] T. Damour, and A. M. Polyakov, Nuclear Physics B **423**, 532 (1994)
[5] G. A. Palma, P. Brax, A. C. Davis, and C. van de Bruck, Phys. Rev. D **68** 123519 (2003)
[6] E. G. Adelberger et al., Prog. in Particle and Nuclear Physics **62**, 102 (2009)
[7] P. G. Roll, R. Krotkov, and R. H. Dicke, Ann. Phys. (N. Y.) **26**, 442 (1964)
[8] V. B. Braginski, and V. I. Panov, Sov. Phys. J. E. T. P. **34**, 463 (1972)
[9] G. M. Keiser, and J. E. Faller, Proc. $2^n d$ Marcel Grossman Meeting on General Relativity", p.696 (1982)
[10] Y. Su et al., Phys. Rev. D **50**, 3614, (1994)
[11] S. Schlamminger et al., Phys. Rev. Lett. **100**, 041101 (2008)
[12] T. Damour, F. Piazza, and G. Veneziano, Phys. Rev. Lett. **89**, 081601 (2002)
[13] J. Khoury, and A. Weltman, Phys. Rev. Lett. **93**, 171104 (2004); Phys. Rev. D **69**, 044026 (2004)
[14] K. A. Olive, and M. Pospelov, Phys. Rev. D **77**, 043524 (2008)
[15] P. Brax, C. van de Bruck, A. C. Davis, J. Khoury, and A. Weltman, Phys. Rev. D **70**, 123518 (2004)
[16] D. F. Mota, and D. J. Shaw, Phys. Rev. D **75**, 063501 (2007)
[17] L. Hui, A. Nicolis, and C. W. Stubbs, Phys. Rev. D **80**, 104002 (2009)
[18] A. Papapetrou, Proc. R. Soc. London A **209**, 248 (1951); E. Corinaldesi, and A. Papapetrou, Proc. R. Soc. London A **209**, 259 (1951); W. G. Dixon, Proc. R. Soc. London A **314**, 499 (1970)
[19] C. M. Will, Living Rev. Relativity **17**, 4 (2014)
[20] R. Wald, Phys. Rev. D **6**, 406 (1972)
[21] S. Isoyama, L. Barack, S. R. Dolan, A. Le Tiec, H. Nakano, A. G. Shah, T. Tanaka, N. Warburton, Phys. Rev. Lett. **113**, 161101 (2014); S. R. Dolan, N. Warburton, A. I. Harte, A. Le Tiec, B. Wardell, L. Barack, Phys. Rev. D **89**, 064011 (2014); S. Akcay, L. Barack, T. Damour, N. Sago, Phys. Rev. D **86**, 104041 (2012); L. Barack and N. Sago, Phys. Rev. D **83**, 084023 (2011); L. Barack and N. Sago, Phys. Rev. D **81**, 084021 (2010)
[22] H. C. Ohanian, American Journal of Physics, **45**, 903 (1977)
[23] J. Khoury, Class. Quantum Grav. **30**, 21 (2013)
[24] N. Gumerov, and R. Duraiswami, J. Acoust. Soc. Am. **112**, 2688 (2002)

[25] N. Gumerov, and R. Duraiswami, SIAM J. Sci. Comput. **25**, 1344 (2003)
[26] G. Kristensson, Course of Electromagnetic Wave Propagation, Faculty of Engineering, Lund University (2008)
[27] T.T. Chen, Dyadic Green Functions in Electromagnetic Theory, 2^{nd}ed., IEEE Press, New York (1994)
[28] T. Heubrandtner, and B. Schnizer, and C. Lippmann, and W. Riegler, CERN-OPEN-2001-074, CERN, October (2001)
[29] F.B. Jensen, and W.A. Kuperman, and M.B. Porter, and H. Schmidt, Computational Ocean Acoustics, 2^{nd}ed., Springer, New York (2011)
[30] J. Bruning, and Y. & Lo, IEEE Trans. Antennas Propagat., **19**, 378-390 (1971)
[31] E. G. Adelberger et al., Phys. Rev. D **42**, 3267 (1990).
[32] S. J. Landau et al., Astropart. Phys. **35**, 377-382 (2012)
[33] W. Hu, and I. Sawicky, Phys. Rev. D **76**, 064004 (2007); T. Faulkner, M. Tegmark, E. F. Bunn, and Y. Mao, Phys. Rev. D **76**, 063505 (2007); S. Capozziello, and S. Tsujikawa, Phys. Rev. D **77**, 107501 (2008); P. Brax, and C. van de Bruck, and A.C. Davis and D.J. Shaw, Phys.Rev. D **78**, 104021 (2008); L. Lombriser, F. Simpson, and A. Mead, Phys. Rev. Lett. **114**, 251101 (2015)
[34] P. Hamilton, M. Jaffe, P. Haslinger, et al., Science **349**, 849 (2015)
[35] A. Upadhye, Phys. Rev. D **86**, 102003 (2012)
[36] V. Anastassopoulos, M. Arik, S. Aune, et al., Phys. Lett. B **749**, 172 (2015)
[37] J. H. Steffen, A. Upadhye, A. Baumbaugh, et al., Phys. Rev. Lett. **105**, 261803 (2010)
[38] T. Jenke, G. Cronenberg, J. Burgdörfer, et al., Phys. Rev. Lett. **112**, 151105 (2014)
[39] T. W. Murphy, Reports on Progress in Physics **76**, 076901 (2013)
[40] C. Burrage, E. J. Copeland, & E. A. Hinds, Journal of Cosmology and Astroparticle Physics **3**, 042 (2015)